REPUBLIC OF IRAQ
MINISTRY OF HIGHER EDUCATION
AND SCIENTIFIC RESEARCH
AL-FURAT AL-AWSAT TECHNICAL UNIVERSITY

Investigation the Performance of Underwater Optical Wireless Communication Under Impacts of Different Modulation Schemes and MIMO Configuration

A THESIS
SUBMITTED TO THE COMMUNICATIONS TECHNIQUES ENGINEERING DEPARTMENT
IN PARTIAL FULFILLMENT OF THE REQUIREMENTS FOR THE DEGREE OF TECHNICAL MASTER
IN COMMUNICATION ENGINEERING

BY

MONTHER NOAMAN HASAN

(B. Sc. Communication Techniques Engineering)

Supervised by

Assist. Prof.

PhD. Ahmed Ghanim Wadday

Sept. 2020

بسم الله الرحمن الرحيم

(ويَسْأَلُونَكَ عَنِ ٱلرُّوحِ قُلِ ٱلرُّوحُ مِنْ أَمْرِ رَبِّي وَمَآ أُوتِيتُم مِّنَ ٱلْعِلْمِ إِلاَّ قَلِيلاً)

صدق الله العلي العظيم

[سورة الاسراء: 85]

Dedication

To the greatest person that Allah has ever created, **Prophet Mohammad** peace be on him and his family.

To the best person that Allah has ever created after His Prophet, **Imam Ali** peace be upon him.

To those who have all the credit on me, to those who were the cause of my existence, to my beloved **parent**.

To my **wife**, my **brothers** and my **friends**...

To all who supported and encouraged me to achieve my success.

Supervisor's Certification

I certify that the thesis titled **" Design and Evaluation Study of Optical Wireless Sensors Networks for Underwater Monitoring System "** which is submitted by **MONTHER NOAMAN HASAN** prepared under my supervision at the Communication Techniques Engineering Department, Engineering Technical College-Najaf, AL-Furat Al-Awsat Technical University, in partial fulfillment of the requirements for the degree of Technical Master in Communication Engineering.

Signature:
Name: **Dr. Ahmed Ghanim Wadday**
Degree: Assistant Prof.
Date: / / 2020

In view of the available recommendation, I forward this thesis for debate by the examining committee.

Signature:
Name: **Dr. Salim Muhsin Wadi**
(Head of communication Tech. Eng. Dept.)
Date: / / 2020

Committee Report

We certify that we have read the thesis titled " **Investigation the Performance of Underwater Optical Wireless Communication Under Impacts of Different Modulation Schemes and MIMO Configuration**" submitted by **MONTHER NOAMAN HASAN** and as an Examining Committee, examined the student's thesis in its contents. In our opinion, it is adequate for an award of a degree of Technical Master in Communication Engineering.

Signature:
Name: **Dr. Ahmed Ghanim Wadday**
Degree: Assistant Prof.
(Supervisor)
Date: / / 2020

Signature:
Name: **Dr. Haider Jabber Abd**
Degree: Assistant Prof.
(Member)
Date: / / 2020

Signature:
Name: **Dr. Ahmed Al Hilli**
Degree: Lecturer

(Member)
Date: / / 2020

Signature:
Name: **Dr. Hayder Jawad Mohammed Albattat**
Degree: Assistant Prof.

(Chairman)
Date: / / 2020

Approval of the Engineering Technical College- Najaf

Signature:
Name: Assistant Prof. **Dr. Hassanain G. Hameed**
Dean of Engineering Technical College- Najaf
Date: / / 2020

Acknowledgment

In the name of Allah, the Most Gracious and the Most Merciful.

All praises to Allah for the strengths and His blessing in completing this work and pleased me the science way, and prayers and peace be upon his Prophet Muhammad and his family (my great teachers).

First of all, I would like to express my warm thanks to my supervisor assistant Prof. Dr. **Ahmed Ghanim Wadday** for providing me the possibility to do a very interesting work.

Sincere thanks going to all the professors at Al-Furat Al-Awsat Technical University /Engineering Technical College Najaf for all this huge basis of information in the academic terms which it was as the foundation stone of this work. Especially who push me and guided me (to name a few: Dr. **Ghufran Mahdi**, Assistant Prof. **Ali m. Alsahlany**, Dr. **Nasser Hussein** and many others).

I would like to thank and appreciate Dr. **Hasan M. Azzawi** for his continuous help and support.

Further thanks are due to my gorgeous family members especially my wife for giving me so much support, love and advice. Without their continuous support and encouragement, this work would not have been completed.

Abstract

The growing requirements for high-speed data transmission and a huge volume of data in underwater applications are significantly advantage from Underwater Optical Wireless Communication (UOWC) systems. Therefore, the development of novel and reliable UOWC systems and the improvement of the existing ones have been a very popular research area in the last decades. Accordingly, my thesis aims to study the design and performance evaluation of the physical aspects of UOWC systems under different modulation schemes and different underwater channels.

The study has investigated different UOWC systems that use the Differential Phase Shift Keying (DPSK) modulation with Direct Detection (DD) Optical Orthogonal Frequency Division Multiplexing DPSK-DD-Optical OFDM and the DPSK modulation with Coherent Detection (CD) technologies Optical Orthogonal Frequency Division Multiplexing DPSK-CD-Optical OFDM. The two schemes are based on different configurations of Multi-Input Multi-Output (MIMO) technology (1×1SISO,1×4SIMO,1×2SIMO,2×1 MISO,4×1MISO, 2×2MIMO and 4×4MIMO respectively) to improve the receiver sensitivity and increasing link range.

Optisystem^{TM} (Ver.16.0.0) is used for simulation of the proposed DPSK-DD-OFDM and DPSK-CD-OFDM approaches with different configurations of the MIMO technique. The simulation results at different conditions show that the performance of DPSK- CD-Optical OFDM is better than DPSK-DD-Optical OFDM scheme by using 4×4MIMO for reliable link range at target Bit Error Rates (BERs) 10^{-5} which less than the threshold of the Forward Error Correction (FEC) which be assumed 10^{-3}. For instance, with DPSK-DD-Optical OFDM system, the link ranges are 10.5m, 31m, and 131m for turbid, mid, and clear water receptively, while with proposed DPSK- CD-Optical OFDM system the ranges are 12m, 38.5m, and 156m for turbid, mid, and clear water receptively. Moreover,

the results also state that the proposed technique revealed better enhancement compared to previous work at the same input parameters.

Table of Contents

Chapter One: Introduction and Literature Review

Chapter Two: Theoretical Background

Chapter Three: System Design

Chapter Four: Simulation Results and Analysis

Chapter Five: Conclusions and Suggestions for Future Works

List of Abbreviations

Symbol	Description
ASK	Amplitude Shift Keying
AUV	Autonomous Underwater Vehicle
BER	Bit Error Rate
BPSK	Binary Phase Shift Keying
CD	Coherent Detection
CDOM	Colored Dissolved Organic Materials
CD-Optical OFDM	Coherent Detection Optical Orthogonal Frequency Division Multiplexing
DAB	Digital Audio Broadcasting
DAC	Digital to Analogue Convertor
DD-Optical OFDM	Direct Detection Optical Orthogonal Frequency Division Multiplexing
DP	Dual Polarization
DPSK	Differential Phase Shift Keying
DVB	Digital Video Broadcasting
E/O	Electrical to Optical Conversion
FDM	Frequency Division Multiplexing
FFT	Fast Fourier Transform
FOV	Field of View
FSK	Frequency Shift Keying
FSO	Free Space Optical
IC	Integrated Circuit
IF	Intermediate Frequency
IM	Intensity Modulation
LD	Laser Diode

LED	Light Emitting Diode
LO	Local Oscillator
LOS	Line of Sight
LPF	Low-Pass Filter
MCM	Multi-Carrier Modulation
MIMO	Multiple In Multiple Out
MISO	Multiple In Single Out
MZM	Mach-Zehnder Modulator
NLOS	Non-Line of Sight
NRZ	Non-Return to Zero
O/E	Optical to Electrical Conversion
OFDM	Orthogonal Frequency Division Multiplexing
OOK	On-Off Keying
OSNR	Optical Signal-To-Noise Ratio
OTR	Optical-To-RF Downconverter
P/S	Parallel to Serial Converter
PAPR	Peak to Average Power Ratio
PIN	Positive-Intrinsic-Negative
POMUX	Polarization Multiplexing
PSK	Phase Shift Keying
QAM	Quadrature Amplitude Modulation
QPSK	Quadrature Phase Shift Keying
RF	Radio Frequency
RZ	Return to Zero
RTO	RF-To-Optical Upconverter
S/P	Serial to Parallel Converter
SISO	Single Input Single Output
SIMO	Single Input Multiple Output
UWC	Underwater Wireless Channel

UWSN	Underwater Wireless Sensor Network
UAWC	Underwater Acoustic Wireless Communication
UOWC	Underwater Optical Wireless Communication
VLSI	Very Large-Scale Integration
WLAN	Wireless Local Area Networks

Nomenclatures

Symbol	Definition
$a_{cl}(\lambda)$	The Absorption Chlorophyll Acid Coefficient
$a_f(\lambda)$	The Fulvic Acid Absorption Coefficient
$a_h(\lambda)$	The Humic Acid Absorption Coefficient
$a_w(\lambda)$	The Absorption Coefficient of Water
$A_o(t)$	Optical OFDM Signal
A_e (t)	Received Electrical Signal
A_R	The Modulated Amplitude of Received Signal
A_{LO}	The Amplitude of Local Oscillator Signal
B	Bandwidth
$b_l^o(\lambda)$	Scattering from Large Particles
$b_s^o(\lambda)$	Scattering From small Particles
$b_w(\lambda)$	Linear Combination of The Scattering Coefficient
C	Channel Capacity
$C(\lambda)$	The Total Extinction in Water
C_S	Concertation of small particles
C_l	Concertation of large particles
E_R	The Received Signal
E_{LO}	The Local Oscillator Signal
f	Frequency
h_e	Impulse Response
I_{dc}	Dark Current
PBG	Background Noise Power
PBG_{sol}	Solar Background Noise Power
$PBG\_{Blackbody}$	Blackbody Noise Power

P_{LO}	The Received Optical Power
P_R	The Local Oscillator Power
P_T	Total Power
$\Re$	Responsivity
R_L	Load Resistance
T_e	Equivalent Temperature
V_π	Voltage of Modulator
$\alpha(\lambda)$	Absorption
$\beta(\lambda)$	Scattering
Δf	Subcarriers Spacing
Δ_λ	The Optical Filter Bandwidth
Λ	Wavelength
θ_0	The Laser Beam Divergence Angle

List of Figures

List of Tables

List of Publications

- Monther Noaman Hasan, Ahmed Ghanim Wadday and Faris M. Ali "Performance Analysis of Underwater Optical Wireless Communication Systems Based on CD-Optical OFDM and Various Subcarriers Indexes", Al-Furat Journal of Innovations in Electronics and computer Engineering (FJIECE), Vol.1 No.01 (30 March-2020), Page No. 24 - 29,"published".

- Monther Noaman Hasan, Ahmed Ghanim Wadday, Faris M. Ali & Hasan M. Azzawi "Performance Evaluating of DD-OFDM based on MIMO System for Underwater Wireless Optical Communications", Test Engineering & Management, Vol.83, Issue March-April (30 April-2020), Page No. 25589 - 25598," published ".

CHAPTER ONE

INTRODUCTION AND LITERATURE REVIEW

1.1 Background

Two-thirds of our Earth is covered with water, the Earth is a water planet. With the rapid technological developments, the area of underwater communications has grown rapidly and widely with wide-ranging applications in many fields such as military and commercial sections, such as remote monitoring in the offshore oil industry, pollution control in environmental systems, scientific data collection from ocean base stations, disaster detection and early warning, national safety, and security (intruding detection and underwater surveillance). The studies into modern underwater wireless communication technologies have thus played a crucial role in the ocean and other marine environments [1]. The underwater wireless channels may be extremely affected by many factors such as marine environment, attenuation, limited power, bandwidth, and frequency dispersion, making the underwater wireless channel is one of the toughest and most complex. When confronted with these unique conditions in different underwater applications, many new challenges that were not faced in wireless terrestrial communications rise for upcoming wireless underwater networks in acoustic, (Radiofrequency) RF, and optical communications. In acoustics and optical systems, because of the opportunity for long transmission distance and high-bandwidth network communications in size, power enabled modems and unmanned systems are among these challenges [1]. The underwater wireless networks have engaged and increased the attention of investigators, not only in the education field but in the military and manufacturing sectors as well, based on their attractive and unique elements as well as the potential advantages of advanced underwater communications. lately, much researches have been done on the underwater wireless networks, but further developments on the wireless

system underwater continue to be a problem, given the previous challenges posed by the exploitation of acoustic and optical wireless channels [2].

There are three possible methods for underwater communications [2]:

- Acoustic by sending sound waves.
- Radiofrequency transmission via electromagnetic waves.
- Optical communication via sending optical carriers.

Each of these approaches possesses benefits and weaknesses.

Acoustic propagation in underwater is affected by high noise level, high latency, path loss, multi-path, high bit error data rate, and bandwidth restricted depending on range and frequency [3]. Furthermore, acoustic communication is not best used underwater particularly for applications requiring high data rates, and real-time surveillance.

For RF carriers, they suffer from high underwater attenuation and require large antennas and high transmission power at low frequencies, this is not feasible underwater.

Optical carriers are electromagnetic waves between 400 nm (blue light) and 700 nm (red light) of wavelength. Because of its wavelength is very short, high frequency, and high speed, optical waves are capable of communicating at the extremely high data rate (up to 1Gbps) [3]. The optical waves used as wireless communication carriers, though, are usually very short due to strong water absorption and strong backscatter of suspended particles in the optical frequency band. Underwater optical communications due to the high data rate, high bandwidth, are a feasible solution. The absorption and dispersion affect the optical propagation path. Table 1.1 depict a comparison among the three techniques [4].

Table-1.1: Comparison Among Acoustic, RF, and Optical Techniques [4].

Parameters	Acoustic	RF	Optical
Transmission Power	10 W	mW-W	mW-W
speed	1500 ms^{-1}	$2.3x10^8$ ms^{-1}	$2.3x10^8$ ms^{-1}
Data Rate	Kbps	Mbps	Gbps
Latency	High	Moderate	Low
Attenuation	0.1 – 4 dBm/Km	3.5 - 5 dBm/m	0.39dB/m (ocean) 11 dB/m (turbid)
Bandwidth	1-100 KHz	MHz	150 MHz
Link range	more than 100 Km	Up to 10 m	10-150 m
Performance Dependency	Temperature, salinity, and pressure	Conductivity and permittivity	Scattering, absorption, and turbulence

1.2 Sensing in Underwater Environments

Sensing is a method used to collect information about a physical entity or process including the occurrence of events such as changes in a condition like temperature drop or pressure drop. The device which performs the task of sensing is called a sensor. For example, the sensors given to the human body collecting visual information from the environment (eyes), acoustic information such as sounds (ears), and smells (nose) [5].

Underwater Wireless Sensor Networks (UWSNs) have been considered as a viable framework for network system. Fig. 1.1 illustrates the UWSN network architecture's is composed of many components. The key components are the sensors. The sensors are the nodes with modems in UWSNs, and are distributed either in shallow or deep water. Sensor node may sense (many sensors can sense specific information about the environment, such as water quality, temperature, pressure, metal, and chemical and biological elements), relay, and forward data.

The data should be passed on to the basic component(s) on the water surface, called surface gateway (sink). The surface gateway must forward data (through radio channels) to the remote-control center. The control center is also on the seashore and oversees the water areas. The control center gathers, analyzes and manages water zone information. The deep-water Autonomous Underwater Vehicles (AUVs) can also be an optional part of a UWSN. The AUVs can assist in data collection and forwarding [6].

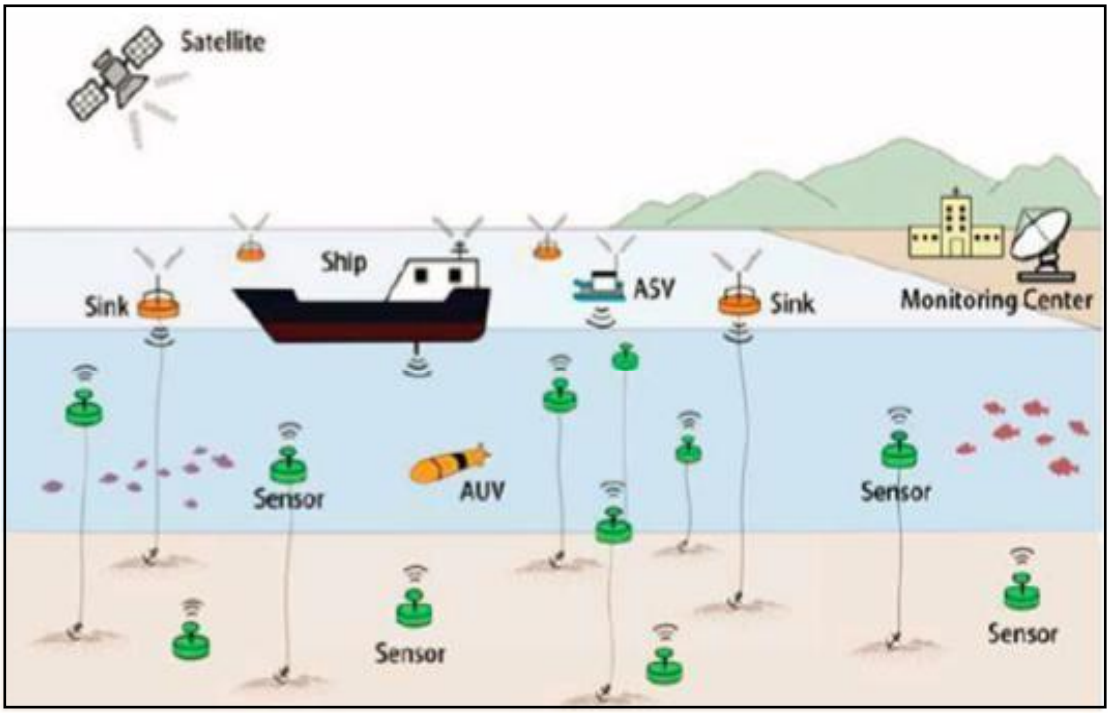

Fig .1.1 Underwater Wireless Sensor Network Structure [6].

This form of UWSN has received increased attention during the last decade, motivated by a great many sciences, military and trade interests, as this could permit a wide variety of applications including: (a) Environmental surveillance: UWSNs can carry out pollution or biological monitoring and can even help predict climate change and weather forecasting, (b) Seismic surveillance: It is extremely important to monitor seismic activities in underwater oil extraction

facilities, (c) Prevention of disasters: A UWSN can issue tsunami warnings for coastal regions by conducting seismic monitoring, and (d) Underwater exploitation: UWSNs may support the exploration, for example, bathymetry profiling and underwater vehicle navigation [7].

These types of applications may produce a large amount of data and the wireless sensor must be able to transmit this information. UOWC can provide unparalleled high data rates and low latency for moderate link ranges, because of the high propagation speed of light waves. It provides safe transmission and is robust to the propagation of multiple paths.

In classical underwater wireless systems, the acoustic carriers are the most common choice, but acoustic waves have disadvantages which are: (i) limited available bandwidth, (ii) enormous time delay, (iii) high cost of available hardware and (iv) limited battery power because it requires high power consumption duo to large transmission antenna for small sound frequency. Although the acoustic wave communication in underwater environments is presently state-of-the-art, its small data rates and its limited bandwidth [8].

1.2.1 Underwater Sensing Problems

In recent years, considerable attention has been given to the problem of underwater target detection and classification in the underwater sensing system. Due to variations in operational and environmental conditions, the presence of varying spatial clutter, differences in the target shapes, compositions, and orientation. This problem is complex. Usually, the target will be identified and classified based on environmental observations with a single sensor (sonar, lidar, etc.) [8]. The sensor from these observations will make a local choice and transfer it to a central station or record the whole sonar image at the central station for post-mission analysis. The problem with sensor-based detection is that the process of detection is limited to only one field. This makes it particularly difficult to

detect weak targets. In addition, in terms of aspect, grassing angles and sonar distance, the structure of targets within an image differs, making detection difficult, especially if this target is in an adverse position with the sensor, e.g. partially obscured targets. Consequently, any improvement in detection results is hampered by the limited amount of data and environmental observations [8].

Distributed sensor networks offer a solution to treat single sensor situations deficiencies. Multiple sensors make it possible to capture the target properties significantly better because the targets are viewed from different aspects, ranges, frequencies, sensor modalities, and so on. In the monitoring area, several transmitters, autonomous underwater

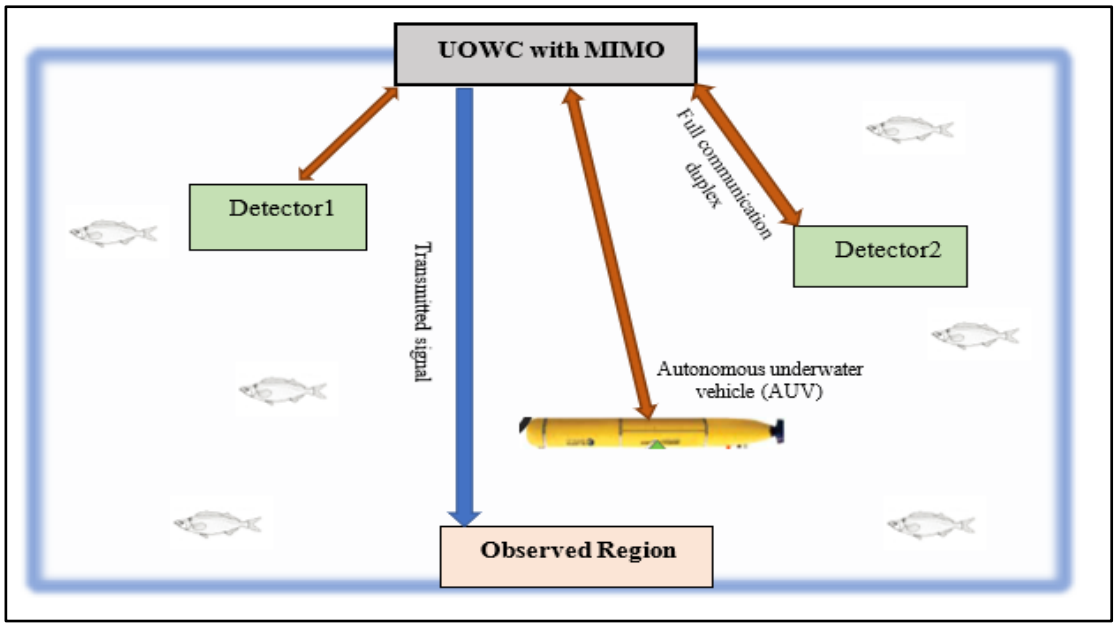

Fig .1 2: UOWC with MIMO for Sensing Application [10].

vehicles, everyone with an inclusive range of sensors including different types of sonars, magnetics, or electro-optical systems may be available (multiple detectors), and multiple detectors as shown in Fig. 1.2:[8].

1.3 Motivation

The UOWC system can be considered as an energy-efficient and cost-effective solving for high data rate and low time latency. The light beams are absorbed, scattered, and faced the multipath effects in underwater propagation, leading to signal deformation in the shape of an Inter- Symbol Interference (ISI) and degrading the total performance of UOWC system. Therefore, a technique which adapts to such a harsh environment is motivated [4].

OFDM-MIMO demonstrate the benefits of wireless communication in the atmosphere. It will be a possible method to utilize in the underwater wireless communication system. MIMO is a widely used multi-optical transmitters and multi-photodetectors technology and serves as an efficacious means to improve significantly systems achievement with respect to increasing data rates and channel capacity [9].

1.4 Problem Statement

UOWC system offers a limitation of the traditional underwater acoustic wireless communications (UAWC) system in an attractive and promising way to address them. Although optical carriers can be utilized to accomplish high data rate communications in Gigabit per second (Gbps), but still suffer from scattering and absorption in water and thus, they are effective only for short-distance communications. These obstacles in UOWC should be addressed to deploy underwater optical networks are transmission length (link range) and underwater attenuation (absorption, scattering, and multipath) [7].

1.5 Literature Review

In the last decades, many researches focused on UOWC systems to handle the problems of underwater propagation. This section presents a review of research conducted on UOWC and some technologies used for underwater applications. This survey can be classified to:

1.5.1 Investigations on Achieving an Initial UOWC

Bin Tian and *et al.* [10], proposed a LED-based UOWC. The power of the LED was 500mW. The maximum communication distance was 30m. The different communication baud rate was used containing 9600 bps, 14400 bps, 19200 bps, and 38400 bps. The experimental finding presents that once transmitting speed increases, the rising time and falling time take more time in one communication clock period and under the baud rate of 19200 bps or less.

P. McGillivray and *et al.* [11], discussed the growth of high repetition rate LED in underwater optical wireless systems and surface and aerial communications for image and data transmission, where the achieved data rate attains 1 Gbps.

Jiemei Wang and *et al.* [12]**,** proposed and experimentally confirmed a long-distance, and high-speed UOWC system in a laboratory environment by utilizing a 520nm LD and modulation type is Non Return to Zero-On Off Keying NRZ-OOK. The scheme was successfully accomplished using a 500 Mbps data rate over a 100 m tap water channel. The measured system BER value was 2.5×10^{-3}.

1.5.2 Investigations of Turbulence, Absorption, and Scattering in UOWC

H. M. Oubei, and *et al.* [13]**,** studied the scintillations of red, green, and blue laser beams in various weak turbulent water channels. The threshold of turbulence in UOWC was learned, and the BER is measured for the green laser,

which shown that the UOWC link can still be retrievable in a turbulent underwater environment if the turbulence was below a certain threshold.

B. Majlesein and *et al*. [14], because of the harsh effects of the underwater environment on the optical wave contain: absorption, turbulence, scattering, and different noise resources, the researchers demonstrated a complete model for UOWC and determine the BER performance and eye diagrams for clear, coastal and turbid waters respectively over an 8 m link range by considering all above effects to calculate the channel impulse response by using Monte Carlo simulation**.**

1.5.3 Investigations on UOWC based on OFDM and/or MIMO technique

I. Mizukoshi and *et al*. [15]**,** used a developed Field Programmable Gate Array (FPGA) platform as a real-time transmitter to implement the UOWC system of 405 nm, data rate 968 Mbps and utilized DD-OFDM over distance 2m under high turbulence environment. The OFDM suffers from large PAPR during transmission was approved.

H. M. Oubei and *et al.* [16], experimentally verified a UOWC using 450nm LD based on (16-QAM-OFDM). The realized data rate was 4.8 Gbps over 5.4m transmission distance under clear water. The acquired results depict that a bit error data rate (BER) of 2.6×10^{-3}, which is below the FEC limits.

Jing Xu and *et al.* [17], proposed and experimentally confirmed a DD-OFDM based UOWC system. The transmitter was a LED of blue wavelength and the receiver was a PIN photodiode (Positive-Intrinsic-Negative). The QAM modulation with different orders and subcarriers was utilized to estimate the underwater bit error rate and optical link range. The transmission link was 40m and performed in coastal. The experimental results showed that the net data rates of 225.9Mb/s at a BER of 1.54×10^{-3} utilizing 16-QAM and 231.95Mb/s at a BER of 3.28×10^{-3} utilizing 32-QAM respectively at 2m link range.

Jing Xu and *et al*. [18], experimentally demonstrated UOWC system using 16-QAM-OFDM and 256-QAM-OFDM modulation OFDM with the support of bit loading using a green LD and a PIN detector, which realizes a data rate of 1.118 Gbps at link range 2m and BER equal to 2.98×10^{-3} under clear water.

Lu Hai Han and *et al.* [19]**,** demonstrated UOWC using a 16-QAM-OFDM modulation technique and utilizing blue LD, the used data rate was 9.6 Gbps was achieved and distance of up to 8 meters under clear water. The feasibility of UOWC for long-distance and high-speed links has been approved by using a two-stage injection-locked technique.

Ho Chun-Ming and *et al.* [20], have indicated that a laser communication system utilizing 16-QAM modulation with an OFDM has achieved an 8.8 Gbps transmission data rate over a transmission distance of 10m based on light injection and optoelectronic feedback techniques.

Yuhang Song and *et al.* [21], suggested and experimentally demonstrated a MIMO-OFDM for the UOWC system, with a bit data rate of 33.691 Mbps channel utilizing blue LED and PIN photodetector over a 2 m water channel. Three systems had been compared (Repetition Coding-OFDM (RC-OFDM), Alamouti-OFDM, and MISO-OFDM) in turbid water. The experimental results showed that the Alamouti-OFDM UWOC is more resistant to delay than the RCOFDM- based system in turbid water.

Mohammad Vahid Jamali and *et al*. [22], accomplished a performance study of the UOWC system using On-Off Keying (OOK) modulation with the MIMO technique (spatial diversity) under coastal water. The simulation results depict that spatial diversity can significantly enhance the system performance duo to mitigate turbulence effect, the MIMO introduces 8dB performance enhancement at the objective BER of 10^{-9} using the 3X1MISO technique under a 25m coastal water link range.

Tsai-Chen Wu and *et al.*[23]**,** experimentally implemented a UOWC in underwater conditions such as clear water and seawater over long distances

utilizing a blue LD and 16-QAM-DD-OFDM data were used to implement the maximum capacity of transmission up to 10 Gbps. The suggested UOWC in clear water provided a permissible range of bit data rate rise from 5.2 to 12.4 Gbps with the matching underwater link range decreased from 10.2 to 1.7m. when implementing the UOWC in seawater (coastal water), there are many attenuation resources such as scattering effects made by impurities. The UOWC bit data rate of up to 7.2 Gbps for satisfied link range further than 6.8m.

Lu I. Cheng and *et al*. [24]**,** proposed and experimentally demonstrated UOWC based on an LED system under turbid water utilizing OFDM and bit loading algorithm. The proposed UOWC realizes 158 Mbps in the daylight and 205 Mbps in the nightlight at a link range of 10m and depth of 3m, also the (BERs) are less than the FEC) threshold (10^{-3}).

Fumin Wang and *et al.* [25]**,** suggested an Underwater Visible Light Communication (UVLC) system using QAM and multi PIN photodetectors. The transmitter was a green 521 nm LED. The proposed system was tested in a 1.3m pool size. They concluded that the ratio of the two receivers can have a significant effect on the system's outputs and can achieve a better communication effect by selecting the appropriate value for it. The data rate was 2.175Gbps.

A. Huang and et al. [26]**,** analyzed the BER performance of the UOWC system using Spatial Modulation (SM) with the MIMO technique. However, the SM achieves high spectral efficiency as compared with convention MIMO using repetition code but the SM requires perfect channel knowledge for data detection because of the differences of wireless links between transmitter and receiver.

Amantayeva Akniyet and *et al* [27], investigated the performance evaluation of the UVLC system utilizing a 2x2 MIMO technique with OFDM under turbid water. By utilizing Weighted Double Gamma Function (WDGF) the channel gain for each path was estimated. To eliminate multiuser interference the researchers implemented a zero-forcing precoding scheme.

Yanlong Li and *et al* [28]**,** proposed the OFDM with imaging lens as a MIMO system to separate the light signal which leads to a decrease in the effects of the underwater wireless communication and achieves 12dB profit at the same bit error data rate as compared with non-imaging MIMO system.

Finally, from the above literature survey, the most relevant investigations to my work are [17],[22]**,** [23]**,** [27].

1.6 Thesis Contribution

The key contributions of this thesis are:

- Using Differential Phase-Shift Keying (DPSK) modulation.
- Performance comparison between Direct Detection (DD-Optical OFDM) and Coherent Detection (CD-Optical OFDM) of UOWC systems.
- Increasing the link range of the UOWC system by using DPSK-CD-Optical OFDM based on the 4×4MIMO technique.

1.7 Thesis Objectives

This study aims to design and performance evaluating of UOWC system to enhance the system performance against underwater limitations, the following objective can be listed:

1. To design and simulate DPSK-Optical OFDM with direct detection and coherent detection based on a 1×1SISO technique.
2. To design and simulate DPSK-Optical OFDM with direct detection and coherent detection based on different a MIMO configuration.
3. To perform the system performance and increase the link ranges under different water types (clear, mid turbulence, and turbid) and the target BERs are 10^{-5}.

4. To compare the proposed work and recent works under same input conditions.

1.8 Thesis Layout

This study is divided into five chapters: -

Chapter1: Presents the background to the UOWC system, sensing in underwater environments, motivation, problem statement, literature review, main contributions, thesis objectives, and thesis layout.

Chapter 2: Gives a general theoretical background such as describing the design of current underwater optical wireless communication technique. Also, it presents the DPSK modulation format, the attenuation in underwater such as turbulence, scattering, absorption, pointing and alignment, multipath interference and dispersion, underwater signal noise sources. In this chapter, the underwater link configurations are presented. Also, this chapter presents basic different types of optical orthogonal frequency division multiplexing (Optical OFDM), and an introduction to the theoretical concepts of the MIMO technique to improve the accomplishment of UOWC system and describes the general mathematical model of the MIMO system.

Chapter 3: Presents the system design and main parameters for the proposed [Direct Detection-Optical OFDM (DD-Optical OFDM) and Coherent Detection Optical OFDM (CD-Optical OFDM) systems] based on different MIMO configurations. The information presented in the previous two chapters is used as a foundation for the design. Also, a brief description of Optisystem™ software will be presented.

Chapter 4: Demonstrates the obtained simulation results for DD-Optical OFDM based on MIMO and CD- Optical OFDM based on MIMO under three types of water (clear, mid, turbid).

Chapter 5: offers the conclusion of the simulation results and recommendations for future work which can improve the performance of the whole technique.

CHAPTER TWO

THEORETICAL BACKGROUND

2.1 Introduction

A typical UOWC system generally consists of two parts are an optical transmitter, and an optical receiver [29]. UOWC system will be reviewed in detail in this chapter and all theories and design considerations are related to it.

2.2 UOWC System Structure

Figure 2.1 illustrates the components of a typical UOWC system. It is a source that generates transmitted information that is modulated on the optical transmitter, which is transmitted at a high data rate at long distances. To focus on the optical beam to the receiver position, the transmitter is provided with a lens. The data-carrying signal can then spread across the underwater channel with geographical location-specific characteristics [29]. At the receiving side, the optical lens collects the received signal for optical-to-electric conversion and proceed it into the photodetector. The electric signal can then be proceeded through a signal processing unit and a demodulator to retrieve the original signal.

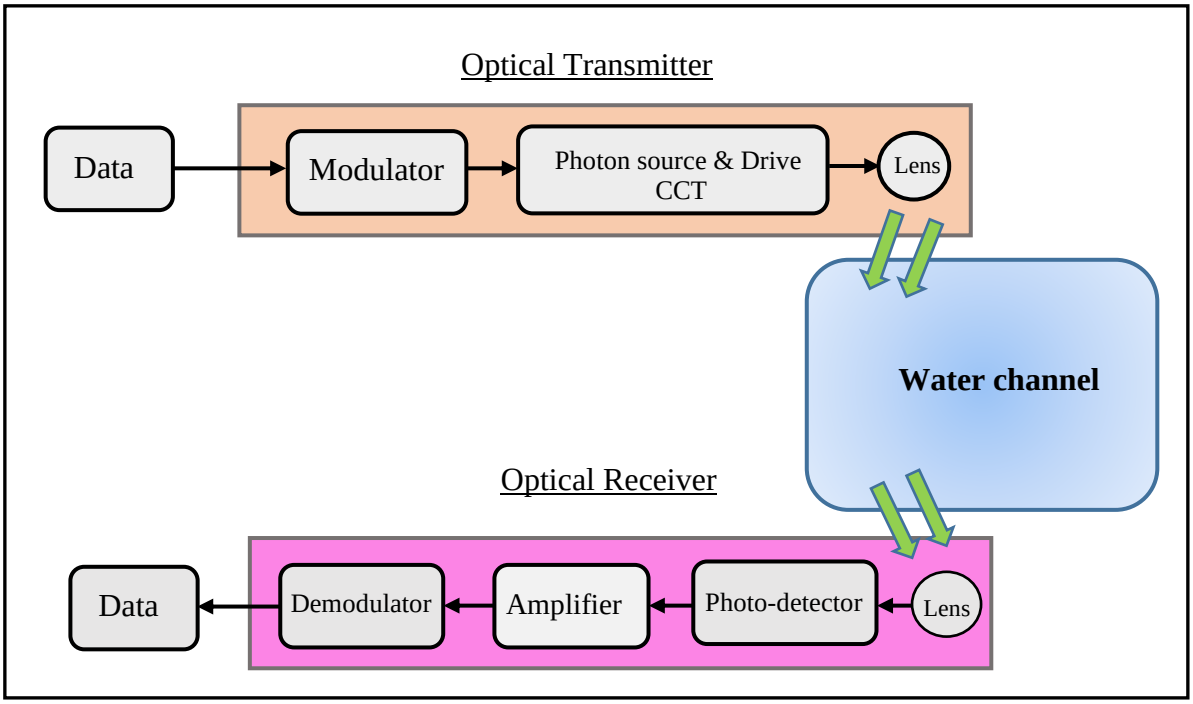

Fig. 2.1: Block Diagram of UOWC System [4].

2.2.1 Optical Transmitter

The electrical data signal is converted into an optical signal, and the optical signal is transformed into a transmission channel. A typical optical transmitter comprising an input signal, an optical system driver, a photon source, and other required light-beam conditioning optics (reflectors and lenses) as shown in Fig. 2.1. [30]. The optical source's function is to transform an electrical input signal into the corresponding optical signal. There are two available types of optical transmitter device based on photon source: Light Emitting Diode (LED) and Laser Diode (LD) [30].

2.2.2 Optical Receiver

An optical receiver's function is to transform the optical signal back into electrical form and to retrieve the data transmitted through the light wave system. The key component is a photodetector that converts light into electricity using a photoelectric effect [32]. It contains an optical signal detector that transforms

into an electric current. Fig. 2.1 shows the system-level receiver design. Two popular examples of photodetector currently in use include Positive-Intrinsic-Negative photodiodes (PIN) and Avalanche Photodiodes (APD) [30,31].

2.2.3 Mach-Zehnder Modulator (MZM)

The MZM is the most commonly used modulator for the external optical modulation. The Mach-Zehnder Interferometer (MZDI) phenomena were discovered by Ernst Mach and Ludwig Zehnder in 1891. In order to reduce the chirp effect, the optical transmitters have been divided into two functions: the first one to generate an optical carrier using a laser diode, the second one to transpose the electrical signal into an optical carrier using an external modulator.

The MZM is composed of two 3dB couplers and two interconnection waveguides with equal length wave to create a Mach-Zehnder Interferometer (MZDI), as shown in Fig. 2.2 and Fig. 2.3. The two waveguides of the MZM are typically fabricated from an electro-optic material such as Lithium Niobate (LiNbO3). In addition, the Gallium Arsenide (GaAs) and Phosphide Indium (InP) are used in the fabrication of the MZM. In an electro-optical material, the refractive index depends on the applied electric field. Thus, an electrical signal can change the refractive index of the crystal which modifies the velocity of the light propagating in the waveguide. Choosing the appropriate level of electrical voltage, the combination of the signals from the two waveguides through the second 3dB coupler can be constructive or destructive. The difference in voltage, which allows moving from a minimum (destructive interference) to a maximum (constructive interference), is known by the voltage of the modulator [37, 38].

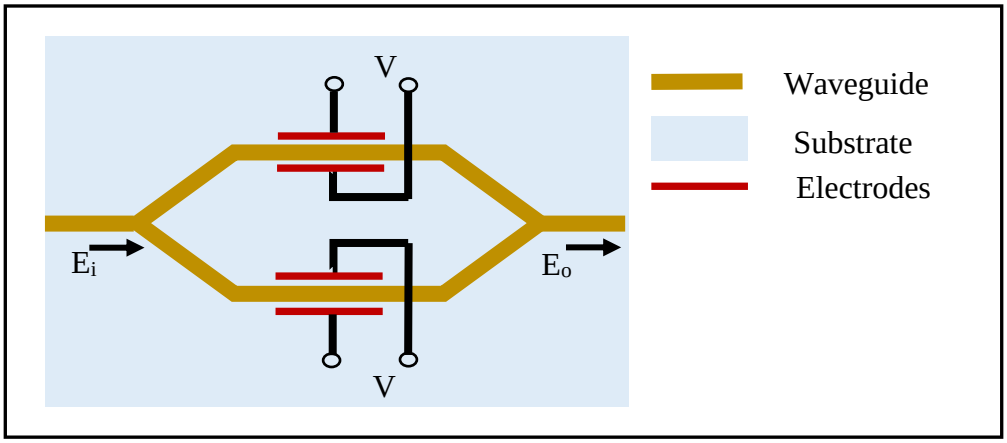

Fig. 2.2: The Output Optical Field of the MZM [37, 38].

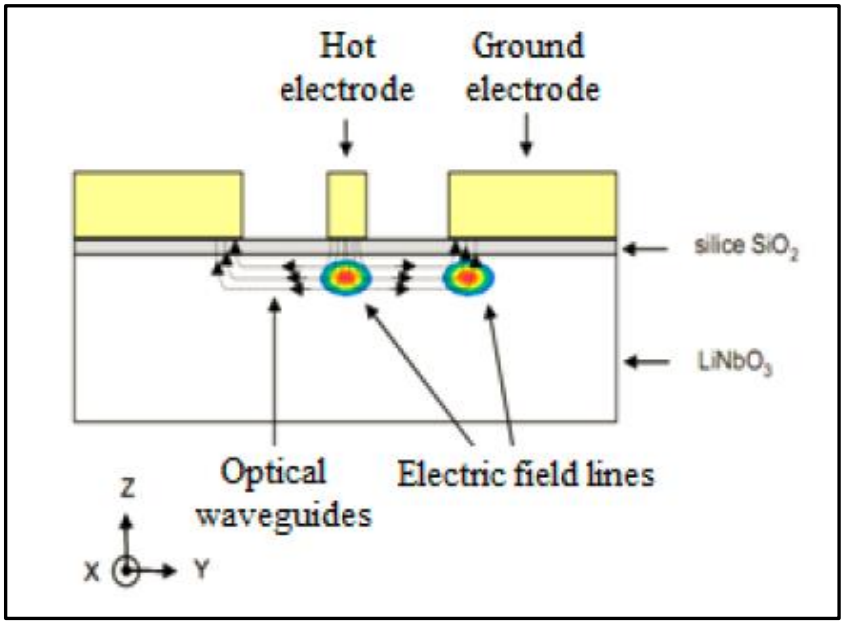

Fig. 2.3: Electrode and optical waveguides placement in the transverse plane [37].

2.3 Modulation Scheme for Optical Communication

In optical communications systems, as well as other digital communications systems, the modulation of a transmitted signal, which modulates information on optical carriers, plays a key role in optical communications systems and other digital communication systems. Modulation formats which employed in optical communication systems are similar to those used in communications systems for radio frequencies, with the frequency, the

phase and the amplitude of information transmitted by an optical wave [35]. In optical modulation technology the information can be modulated on optical carriers and transmitted by optical systems. The digital modulation technology divided into several types of modulated variables, such as Amplitude Shift Keying (ASK) and Phase Shift Keying (PSK) and Frequency Shift Keying (FSK). Based on the modulated variables, the ASK format is the simplest format for modulation. In FSK, a frequency difference occurs around a center frequency, and in PSK the carrier signal phase is shifted by 180° according to the information bit (0,1). In order to modulate signals, polarization states for the Polarization Shift Keying (PolSK) signals can also be utilized beside amplitude, phase, and frequency. In addition, polarizing statements can also be used to multiplex other optical signal types, which produce new signals. Polarization based modulation formats for high bit-rate optical communications networks have been extensively studied in lately years. For next-generation optical networks, multiple levels modulation arrangements such as QAM, which encrypts data in the amplitude and the phase of the optical carrier to further improve spectral efficiency, are also studied and proposed. Several frequently used optical modulation formats will be reviewed together with some advanced ones [35].

2.3.1 Phase Shift Keying (PSK)

Several digital data encoding techniques are available for an analog signal. ASK, FSK and PSK are three basic types. Fig. 2.3; shows the differences between them. In ASK, the carrier frequency is used to send the bits with an amplitude difference. In FSK a frequency difference occurs around a center frequency and the signal phase in PSK is modified, so the binary digits (1,0) are represented by two different phases $(0, \pi)$, the Binary Phase Shift Keying (BPSK) would most likely be the phase shift of the modulation shown below.

The phase difference of the two situations is Ø=π. The expression for the representation of BPSK is [36]:

$$S_t = \begin{cases} A\cos(2\pi f_c\, t) & for\ binary\ 1 \\ A\cos(2\pi f_c\, t + \emptyset) = -A\cos(2\pi f_c\, t) & for\ binary\ 0 \end{cases} \quad (2.1)$$

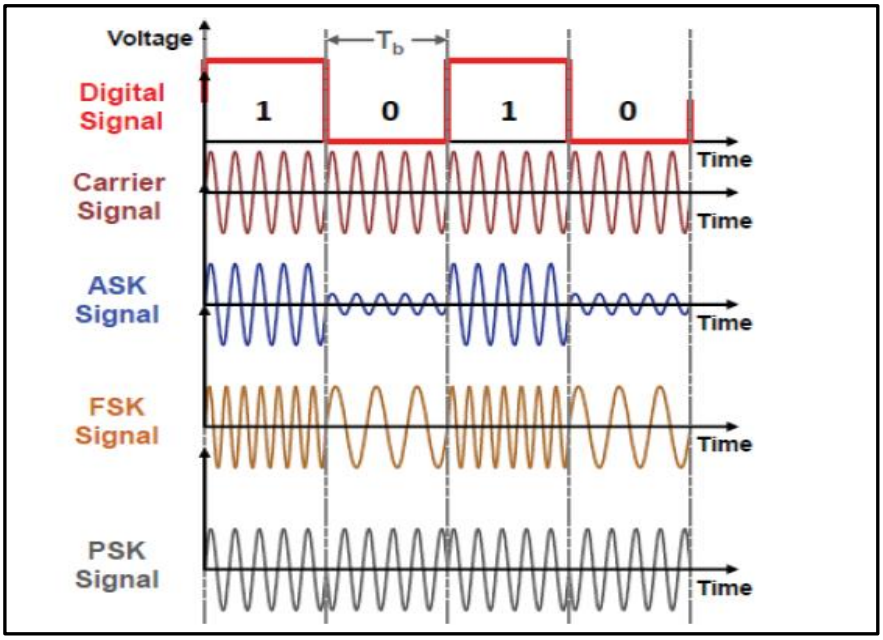

Fig. 2.4: Three Modulation Techniques; ASK, FSK and PSK [36].

2.3.2 Differential Phase Shift Keying (DPSK)

The DPSK modulation could be an alternative to the BPSK modulation [37]. Binary data is encoded in the DPSK signal between the adjacent bits in shifts in both 0 and π phases. For example, a binary 0 bit is represented by the presence of a phase shift of π, while a binary 1 bit is encoded without a phase shift between the adjacent bits as depicting in Fig. 2.4. DPSK offers better sensitivities than On Off Keying (OOK). The difference between the BPSK and the DPSK is that the bits are represented in the DPSK not by a certain phase but by a phase change. When a binary one is sent, the phase stays the same as the previous bit and a binary zero is represented by a phase shift. Compared to PSK, the DPSK scheme has certain preference. Because the information is stored in

phase change between adjacent binary digit instead of in phase itself, it is good for systems that are not aware of the precise phase (phase shift problems). This makes it easier to detect the signal using the DPSK if the system is influenced by phase noise. However, by using DPSK instead of PSK you also lose 3 dB of power [37].

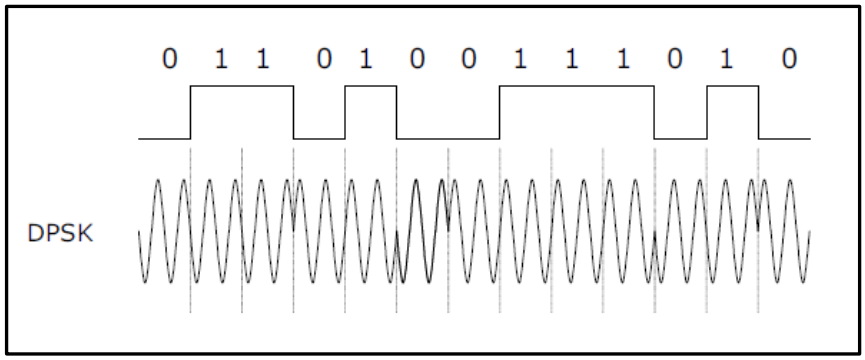

Fig. 2.5: Differential Phase Shift Keying example [37].

The circuit design of DPSK modulator cosists of EXCLUSIVE NOR (XNOR) logic circuit , one bit delay and balanced modulator .An incoming information bit is XNORed with the previous bit prior to entering the balanced modulator as showen in Fig. 2.5 [37].

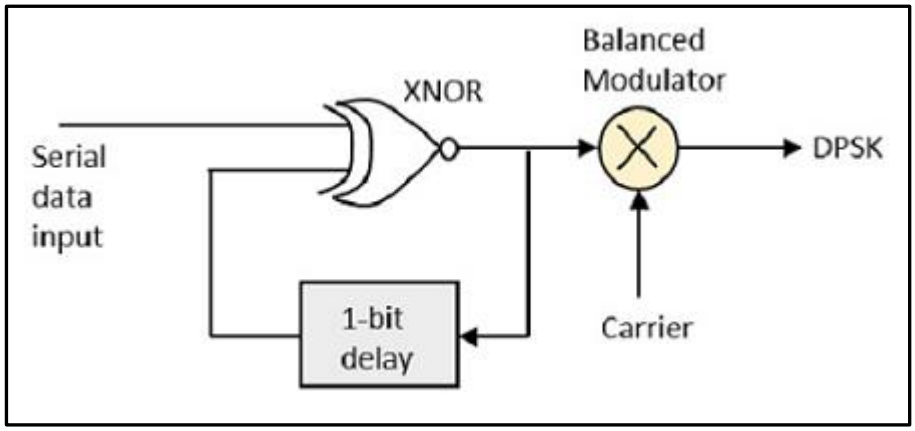

Fig. 2.6: Circuit Design of DPSK modulator [37].

2.4 Factors Affecting in UOWC

Attenuation (absorption and scattering) ,turbulence, alignment, multipath interference, background noise, dark current noise, thermal noise and current shot noise are the critical factors that influence the UOWC systems [4].

2.4.1 Attenuation

The optical signals utilized as wireless communication carriers are usually restricted to very short distances due to extreme water absorption at the band of optical frequencies and heavy back scattering from suspended particles. one of the major drawbacks is the optical waves are generally extremely absorbed in water, the other is the optical diffusion of all particles within the sea. However, in the blue / green region of the visible spectrum ocean water it shows decreased absorption. High speed connection can be achieved depending on the water type (wavelength from 400-500 nm for clear water up to 300-700 nm for turbid water environments) using appropriate wavelength, for example in a blue / green region. The minimum attenuation is concentrated in clear waters at about 460 nm for dirty waters near 540 nm in mid waters and shifts to higher values, as shown in Fig. 2.6 and Table 2.1; [41, 42].

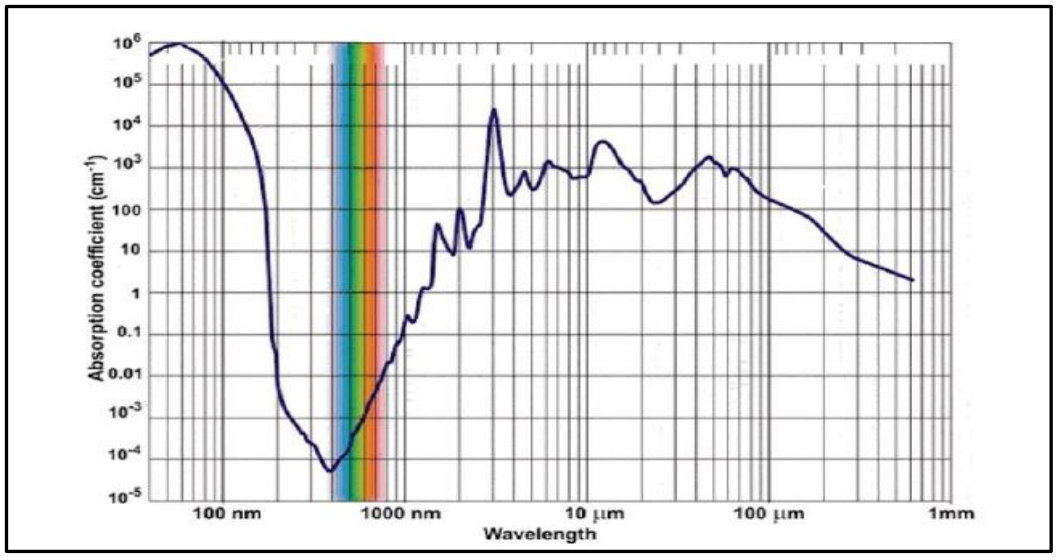

Fig. 2.7: The Transparent Window for Light Aquatic Absorption [38].

Table-2.1: Ideal transmission wavelength for different water types

Water type	Chlorophyll Concertation	Humic and Fulvic Concertation	wavelength	Optical sources wavelength
Pure sea/clear ocean	Less	Less	450-500 nm (blue-green)	LED =521nm LD = 450 nm
Coastal ocean	High	High	520-570 nm (yellow-green)	LED =521nm LD = 450 nm
Turbid harbor	Very high	Very high	520-570 nm (yellow-green)	LED =532 nm LD = 521 nm

2.4.1.1 Absorption

The main phenomenon that result in the loss of intensity of optical signal underwater are absorption as the coefficient of spectral absorption ($\alpha(\lambda)$), which is the difference in the beam of light because the medium is absorbed per meter of the path length. Total absorbance is a linear combination of pure seawater absorption, wave-length and concentration chlorophyll absorption and dissolved organic colored compounds. The division of the yellow substance into two components makes the model universally applicable to all water that is biologically stable and enables future models to more consistently incorporate the effects of fluorescence. The absorption coefficient $\alpha(\lambda)$ is given by:

$$\alpha(\lambda) = a_w(\lambda) + a_{cl}(\lambda) + a_f(\lambda) + a_h(\lambda) \qquad (2.2)$$

where $a_w(\lambda)$ is the absorption coefficient of water as a function of wavelength (m^{-1}) , $a_{cl}(\lambda)$ is the absorption chlorophyll acid coefficient as a function of wavelength, $a_f(\lambda)$ is the fulvic acid absorption coefficient and $a_h(\lambda)$ is the humic acid absorption coefficient both as a function of wavelength [42,44].

2.4.1.2 Scattering

The loss of optical flux due to the re-direction of photons represents the scattering coefficient, $\beta(\lambda)$. The total scattering is a linear combination of the scattering coefficient of water, $b_w(\lambda)$, scattering from small particles, $b_s^o(\lambda)$ as a function of wavelength and concentration, and scattering form large particle, $b_l^o(\lambda)$as a function of wavelength and concentration. The scattering coefficient $\beta(\lambda)$ is specified by:

$$\beta(\lambda) = b_w(\lambda) + b_s^0(\lambda)C_s + b_l^0(\lambda)C_l \qquad (2.3)$$

where C_S is a concentration of small particles and C_l is a concentration of large particles [42, 44].

Eq. 2.5 shows the path loss factor as a function of distance z and wavelength λ [41]

$$\mathrm{L}(\lambda, z) = L_0 e^{-c(\lambda)z} \qquad (2.5)$$

Where $\mathrm{L}(\lambda, z)$ is optical signal power after transmission, L_0 is optical signal power before transmission and $c(\lambda)(m^{-1})$ is the extinction coefficient showing the total attenuation occurred via the underwater propagation. The sum of absorption and scattering represent the total attenuation. The total attenuation coefficient in equation (2.6) which is used in a fully absorbing or totally scattering medium. The absorption coefficient (α) or the scattering coefficient (β), respectively may be replaced. The $C(\lambda)$ z product is also known as the attenuation length and helps to decrease the received power by an exp factor. The extinction coefficient will be based on this [6, 43]:

$$C(\lambda) = \alpha(\lambda) + \beta(\lambda) \qquad (2.6)$$

Where $\alpha(\lambda)$ is the absorption coefficient, $\beta(\lambda)$ is the scattering coefficient, and λ is the wavelength. The typical values of $\alpha(\lambda)$, $\beta(\lambda)$, and $c(\lambda)$ associated with four major water types are given in Table 2.2. Absorption is the main factor for

pure sea water; the low dispersion coefficient frees the beam from divergence. The concentration of dissolved particles in clear ocean water is higher and affects scattering. In coastal ocean water the dominant sources of absorption and scattering are high concentrations of plankton, waste and minerals. The highest concentration of dissolved is found in the turbid harbor water, which seriously reduces light propagation [38]. Table 2.2 depicts standard values for the coefficients (c(λ), α(λ), β(λ)) taking into account the water classification. The three major water types are the following with extinction values:

Table-2.2: Standard values of extinction coefficients (absorption and scattering) [4,41,43].

Water Type	**α(λ) (m^{-1})**	**β(λ) (m^{-1})**	**c(λ) (m^{-1})**
Pure Water	0.053	0.003	0.056
Clear water	0.114	0.037	0.151
Coastal Water	0.179	0.220	0.399
Turbid Water	0.366	1.829	2.195

2.4.2 Turbulence

Variation in the refraction index along the transmission path caused by fluctuations in the underwater environment, salinity, density and temperature leads to large fluctuations in the receiver signal intensity. This fact is called scintillation, and it reduces UOWC 's efficiency. As such, there is no specific model for underwater turbulence as in the case of free space optical (FSO) communication because of the dynamic nature of the underwater environment [4].

2.4.3 Pointing and Alignment

Because of the optical beam is very narrow in UOWC keeping the Line of Sight (LOS) for a dependable underwater link is extremely important. And because of the motion produced by vehicles in underwater, ocean current or other turbulent causes, a continuous tracking between transceivers is quite important to preserve a continuous dependable link. In UOWC the errors of pointing contain two mechanisms: jitter and bore-sight. Jitter is the arbitrary movement of the beam midpoint at the detector plane while bore-sight is a fixed movement between the beam midpoint and the midpoint of the detector [4].

2.4.4 Multipath Interference and Dispersion

multipath interference is generated in an underwater optical channel when an optical wave reaches the detector after coming across multi-scattering stuff or multi reflections from other underwater objects. It ultimately leads to dispersion of waveform time (time spread) and lowers the data rate due to ISI. Nevertheless, the impact of multipath interference in UOWC is not very noticeable in comparison with acoustic communication due to very high light speeds. The volume of interference from multipath depends on system parameters and the propagation environments. Optical waves reflected from the surface or the bottom produce several signals at the detector for shallow water conditions. Such surface and bottom reflections can be overlooked for deep oceans. Advanced signal processing methods like channel equalization and adaptive optics are utilized to minimize interference at the receiver. Although channel equalization for rapidly changing underwater channels appears to be a major challenge, careful characterization of an optical aquatic channel will aid to select correct system design parameters for stable and high-quality optical links [4].

2.4.5 Noise Sources

The underwater optical wireless communication system may be disorganizing by several noise sources. Briefly, we talk about each noise. The noise sources involve (1) background noise, (2) dark current noise, (3) thermal noise, and (4) shot noise [43].

2.4.5.1 Background Noise

The background noise is black body radiation and the underwater ambient light, whose major source is the refracted sunlight from the water surface. The power of background noise can be described as [43] :

$$P_{BG} = P_{BG\_sol} + P_{BG\_blackbody} \quad (2.6)$$

Where, P_{BG_sol} is Solar Background Noise Power and $P_{BG\_blackbody}$ is Blackbody Background Noise Power [43].

2.4.5.2 Dark Current Noise

It is the noise existing at the detector (photodiode) occasionally named photodetector noise [43]. It is a relatively small electrical current that flows across photosensitive devices such as a photodiode even when no photons enter the device; it comprises of the charges produced in the detector when no exterior light enters the detector [43].

2.4.5.3 Thermal Noise

It can be described as the electronic noise produced by the charging carriers' thermal excitation (usually the electrons) within an electrical conductor. A result of the thermal excitement of electrons depends on the bandwidth and temperature of the surroundings [43].

2.4.5.4 Current Shot Noise

Shot noise or Poisson noise is a type of noise that can be modeled by a Poisson process. In electronics, shot noise originates from the discrete nature of the electric charge. Shot noise also occurs in photon counting in optical devices, where shot noise is associated with the particle nature of light. This noise exists when the received signal is presented [43].

2.5 Underwater Link Configurations

There are three essential kinds of underwater optical link configurations [4, 46, 35]: (1) Direct LOS links, (2) Non-LOS links, and (3) Retro-reflector links.

2.5.1 Direct Line of Sight (LoS) Links

Direct LoS link is the simplest, and point-to-point underwater connection between transmitter and receiver, as shown in Fig. 2.8. This connection is quite well established based on static transmitters or receivers, such as two sensor nodes at the bottom of the ocean [4]. Very advanced pointing and tracking mechanisms are required for moveable devices such as autonomous underwater vehicles (AUVs) in order to keep both transmitters and receivers boring [34].

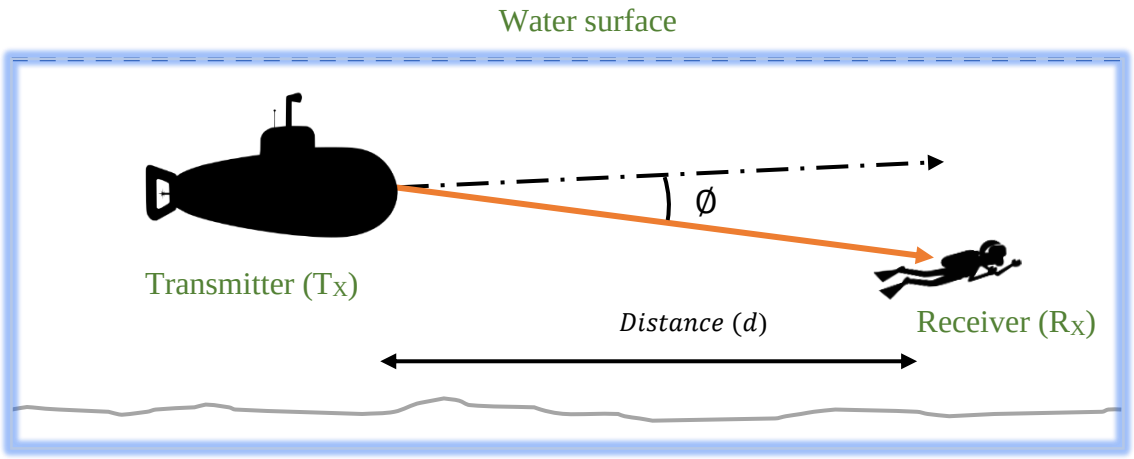

Fig. 2.8: Direct LoS Link Configuration [4].

Where *d* is the perpendicular distance between the transmitter and receiver plane, ∅ is the angle between the perpendicular to the receiver plane and the transmitter-receiver trajectory. It is well functioning in clear oceans where a narrow signal is sent to the recipient by the transmitter. However, because of the growing of the marine life, fish groups or other hurdles, there are high chances of obscuration [39]. Therefore, it is important that a system is developed avoiding marine life from obstructive the propagation route to implement a LoS. Fish of the ocean prefer blue and green wavelengths while fishes of the fresh water prefer wavelengths of yellow and green. Therefore, flashing or erratic lights are favorite to prevent fish from entering the LoS region [4].

2.5.2 Non- Line of Sight (NLoS) Links

NLoS setup solves the LoS UOWC alignment constraint, as shown in Fig. 2.9. The transmitter in this configuration the light beam is projected to the sea surface, with an angle of incidence greater than the critical angle (Q_{max}) [44]. To guarantee the proper receipt of the optical wave, the receptor should continue to face the water surface in a direction approximate to the reflected light.

The key obstacle of the NLoS links are irregular sea surface slopes induced by wind or other turbulence sources. These unwanted phenomena are reflected in the transmitter's light and cause severe signal dispersion, where *h* is transmitter depth and *x* is receiver depth from water surface [46].

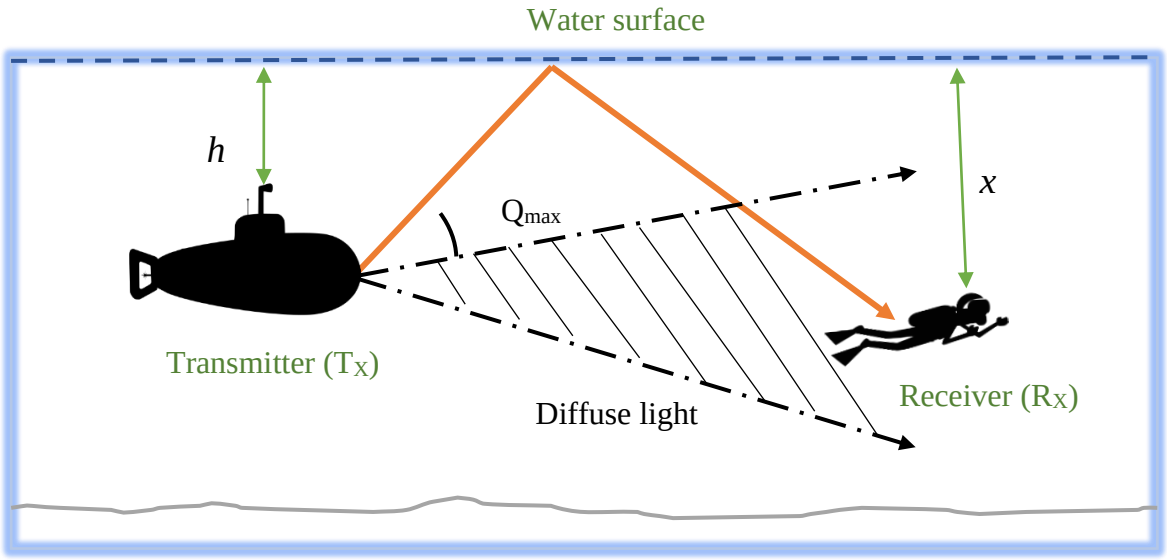

Fig. 2.9: NLOS Link Configuration [44].

2.5.1 Retro-Reflector Links

In restricted duplex communication situation with low capacity of receivers' power to support full transceiver operations, retro-reflectors links are used, as shown in Fig. 2.10. Here, the source has more power and load capability than the receiver; hence, it acts as a transmitter of modulated light signals to the remote receiver. The faraway receiver is fitted with a small optical retro-reflector which mirrors it back to the same source when the incoming beam is sensed from the source, where *h* is transmitter depth and *x* is receiver depth from water surface [4].

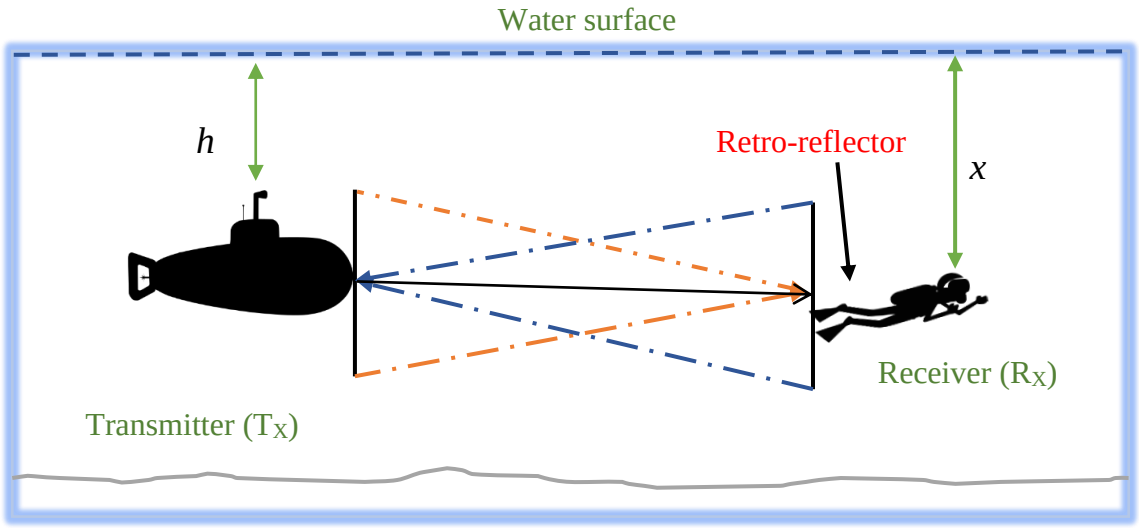

Fig. 2.10: Retro-Reflector Link Configuration [4].

2.6 Turbulence Model in UWOC Channel

Early underwater channel studies often used simple models such as Beer Lambert's law to simulate the propagation of light in underwater. Despite the modification, still Beer Lambert's law cannot fully describe the channel characteristics of UWOC systems since it only includes range dependence, and cannot address the spatial and temporal properties [29].

Underwater turbulence can be divided into three channels, namely weak (clear water), mid water, and strong turbulence (turbid water) based on the value of the beam scintillation index $(\sigma_I^2)$is defined as the normalized variance of the laser irradiance. It's a measure of turbulence strength. Mathematically, scintillation index is defined by [46]:

$$\sigma_I^2 = \frac{E[I^2] - E^2[I]}{E^2[I]} 2 = \frac{E[h^2] - E^2[h]}{E^2[h]} \tag{2.7}$$

where I_0 is the fading-free intensity, and $E[x]$ denoted the expected value of the random variable x. A scintillation index of high value indicates a strong turbulent channel while a scintillation of low value describes a weak turbulent channel. Weak turbulence channel is defined for $\sigma_I^2 \ll 1$. Moderate turbulence

channel is designated as $\sigma_I^2 \sim 1$. Strong fluctuations, also known as the saturation channel c achieved when $\sigma_I^2 \gg 1$.

To design robust and reliable UOWC systems, it is important to investigate and understand the statistical distribution of optical signal fluctuations due to underwater optical turbulence. Early studies on underwater optical turbulence had mostly focused on theoretical investigations based on the formulation of free-space atmospheric turbulence models such as the lognormal distribution to describe the irradiance fluctuations in the underwater environment. However, the spectrum of refractive-index variations caused by temperature or pressure in homogeneities in the atmosphere is much different from the refractive-index spectrum of temperature or salinity in water. This makes the lognormal distribution not appropriate for modeling the irradiance fluctuations in turbulent water. Gamma-gamma distribution has been considered as a candidate for describing the UOWC channel [46].

2.6.1 Gamma-Gamma Model

The Gamma-gamma scintillation model is based on Doubly Stochastic theory and it has weak to strong turbulence condition so the PDF (Probability Density Function) of its intensity (*I*) is product of two gamma random variables which represents fluctuations from small and large turbulence. The two random variables are *X* and *Y* and the received intensity *I*, is [47]:

$$I = XY \tag{2.8}$$

The PDF of *I* is:

$$P(I) = \frac{2(ab)^{(a+b)/2}}{\Gamma(a)\,\Gamma(b)} \times I^{\left(\frac{(a+b)}{2}\right)-1} \times K_{a-b}\left(2\sqrt{abI}\right), I > 0 \tag{2.9}$$

Where: *I* is irradiance, *Γ(.)* is gamma function, and *K(a,b)* is Bessel function of second order. The (a and b) are numbers of small and large turbulence cells and given by [47]:

$$a = \frac{1}{exp\left[\frac{0.4\sigma^2}{\left(1 + 1.11\sigma^{\frac{12}{5}}\right)^{\frac{7}{6}}}\right] - 1} \tag{2.10}$$

$$b = \frac{1}{exp\left[\frac{0.5\sigma^2}{\left(1 + 0.69\sigma^{\frac{12}{5}}\right)^{\frac{5}{6}}}\right] - 1} \tag{2.11}$$

Where σ^2 represents variance. The scintillation index which is used to describe the quantity of turbulence for channel model is given by[47]:

$$\sigma^2 = \left(\frac{1}{a}\right) + \left(\frac{1}{b}\right) + \left(\frac{1}{ab}\right) \tag{2.12}$$

The Gamma-gamma distribution shows excellent agreement with all ranges of turbulence if no spatial diversity techniques applied to it. But in order to remove turbulence effect spatial diversity is one of the best mitigating technique. The gamma–gamma distribution shows significant results if spatial diversity techniques have no correlation between sub-channels and it can be easily modified in such scenarios [47].

2.7 Fundamentals of OFDM and MIMO Techniques in Optical Communications

After all, while underwater propagation, the light beams are absorbed and dispersed, this leads to signal disruption in the type of Inter Symbol Interference (ISI) and complete performance degradation. Consequently, the technique which adapts to such an environment is motivated. OFDM-MIMO demonstrates the benefits of wireless communication in the atmospheric conditions. It will be a possible method to use in the UOWC system [48].

MIMO is a widely used multi-optical transmitter and photodetector technology and serves as an effective means to increase system performance from where performance and improved data rates. MIMO is the most widely used technology than the standard SISO approach. The MIMO technique provides high data rates besides longer link range and enhances transmission reliability and efficiency. OFDM can be regarded because it is not simply a reasonable solution for reducing ISI but also a low complex approach to be implemented in a real system. OFDM is classified as Multicarrier Modulation (MCM) where the data is transmitted through many lower subcarriers. The two key advantages of OFDM are its usefulness against the channel scattering and its simplicity in a time-varying environment [49].

2.7.1 OFDM Technique

Chang is the first proposed OFDM Principle [48]. Due to the absence of broadband applications for OFDM and the need for effective integrated electronic circuits to sustain complicated processing, OFDM has obtained the most evolved part in military applications. Nevertheless, the development in broadband digital applications and the Very Large-Scale Integration (VLSI) CMOS chips in 1990 brought OFDM into the spotlight. In 1995, OFDM was the first Digital Audio Broadcasting (DAB) standard, and then OFDM became the

most important modulation technique in many standards such as Digital Video Broadcasting (DVB), Wireless Local Area Networks (WLAN), and long-term evolution (LTE) which is the fourth-generation mobile communications technology. However, the advantage of OFDM, to be exact, is its robustness against optical channel dispersion, was not unknown in optical communications until 2005, when Dixon proposed the use of OFDM to solve the modal dispersion in multimode fiber. So, it's not a chance that the primary research in optical OFDM focused on multimode fiber applications. The main interests in optical OFDM are in three fields: OFDM for large distance transmission, Direct-Detection Optical OFDM (DD -Optical OFDM), and Coherent Detection Optical OFDM (CD - Optical OFDM) [51,53].

2.7.1.1 OFDM Basics

In this study, the water channel can have multipath impacts. The modulations mentioned so far suffer a great deal in such an environment and multipath that could even impair communication to a point in which the message is unusable. When multipath impacts are existent, it is necessary to look at more reliable modulations. Currently, OFDM is still considered as a good candidate to be included in these situations. OFDM is a kind of MCM in which a stream of data at one rate is split into many parallel lower rate streams. The streams are separately modulated onto different frequency carriers' waves, or subcarriers, for transmission over the same channel. Recently the OFDM has been utilized to optical communication, nevertheless, in some optical systems inclusive wireless optical, single-mode fiber, multimode optical fiber, and plastic optics, there is a growing amount of documents on the theoretical and practical performance of OFDM.OFDM is considered an improved version of Frequency Division Multiplexing (FDM) [50]. In the FDM scheme, various information is transmitted simultaneously over various frequency carriers for various users as shown in Fig. 2.11. Each subcarrier is equipped with a large guard band at the

transmitter part, after the user's data modulates to avoid it from interfering with the neighboring subcarrier. The guard band, nevertheless, will reduce the system's spectral efficiency. The received signals are then demodulated by oscillator banks at the receiver.

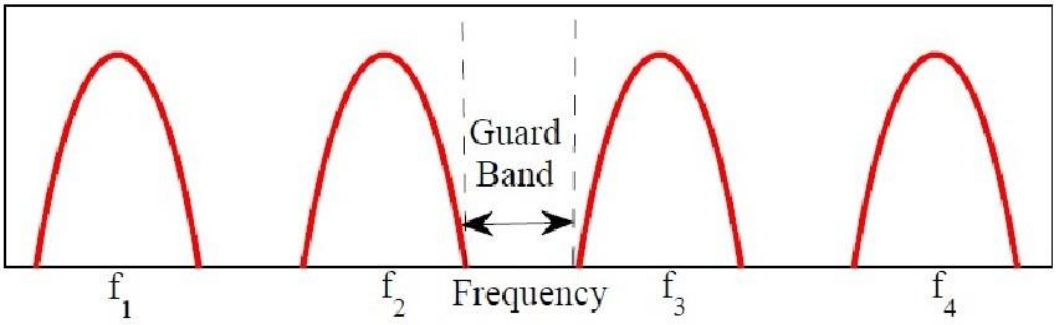

Fig. 2.11: FDM Spectral [54].

In OFDM, as a special case of FDM, OFDM uses many carriers per a given spectrum that are very close to each other, However, they remain orthogonal at an exact distance of each other [50]. The utilize of the Fast Fourier Transform (FFT) and Inverse FFT aid demodulate and create the essential signal even if the subcarriers overlap, as depicted in the Fig. 2.12.

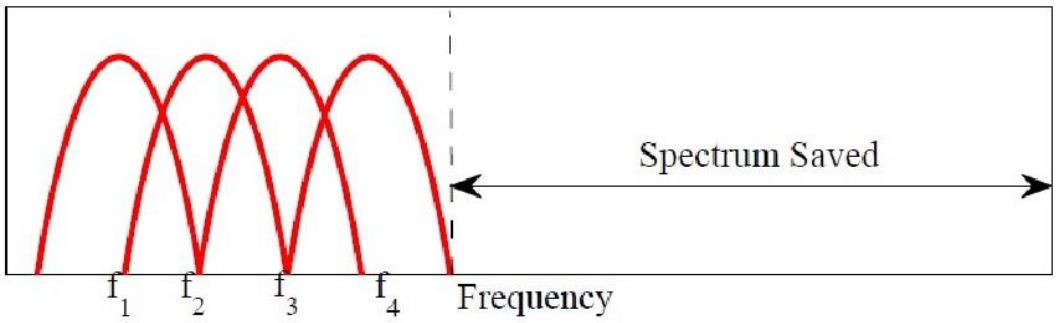

Fig. 2.12: OFDM Spectral [50].

The OFDM signal is generated from a number of sinusoids, each of which corresponds to a subcarrier. Subcarriers can be mathematically represented as [51]:

$$S_k(t) = \begin{cases} \sin(2\pi k \Delta f t), & 0 < t < T, k = 1,2,\ldots,N \\ 0, & otherwise \end{cases} \quad (2.13)$$

Where Δf is the subcarrier spacing, N is the number of subcarriers, and T is the data symbol period. Since the highest frequency component is $N\Delta f$, the transmission bandwidth is approximately $N\Delta f$. Signals are orthogonal if they are mutually independent of each other [51].

These subcarriers are orthogonal to each other because they satisfy the following condition [52]:

$$\int_0^T s_i(t)\, s_j(t) dt = \begin{cases} c, i = j \\ 0, i \neq j \end{cases} \quad (2.14)$$

OFDM signals have the orthogonality property to look at their spectrum. The orthogonal transmission form is the result of each subcarrier 's peak which corresponds to the nulls of all other subcarrier [52].

2.7.1.2 OFDM System Description

Figure 2.13 demonstrates a schematic diagram of the transmitter and receiver of a standard OFDM wireless system. The high data rate digital stream is divided into N parallel streams on the transmitter side by serial to parallel (S/P) conversion [53]. The modulation system (QAM, PSK, QPSK, DPSK, etc.) maps each stream to a symbolic stream. In order to change the OFDM message from a frequency domain to a time domain, the symbols are modulated using IFFT on the sub-carrier. After IFFT, to avoid overlap among sub-band carriers, the cyclic prefix is inserted, then convert the OFDM signal to an analog signal using digital to analog converter. Next, after performing a parallel to serial (P/S) conversion, the signal is sent via a local oscillator through the channel [53].

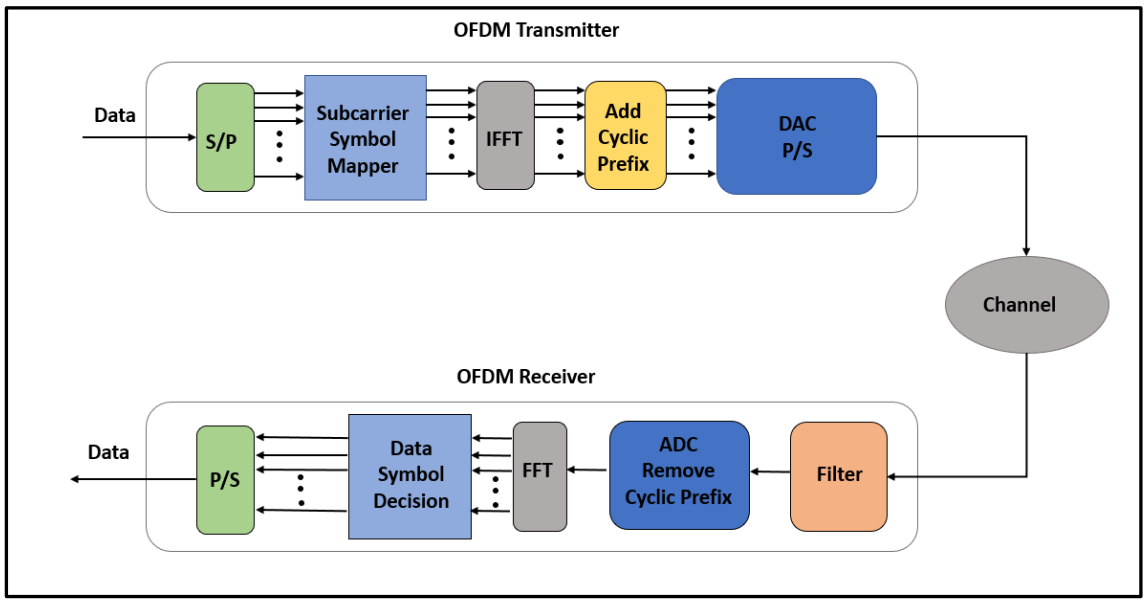

Fig. 2.13: Block Diagram of an OFDM Structure [53].

On the recipient side, by analog to digital converter, the received signal is converted to digital and parallel to remove of the cyclical prefix. The signal will then be demodulated by utilizing the FFT process and demodulated using either the QAM, PSK, or DPSK data symbol decisions. The data is converted to serial for the original data to be obtained [53].

2.7.1.3 OFDM in Optical Communications

In 2005 OFDM was initiated into the optical domain, and have been two essential approaches which allow the demodulation of an optical signal into the electrical signal originally transmitted. The first is the direct detection Optical OFDM (DD-Optical OFDM) and the second is the Coherent Detection Optical OFDM (CD-Optical OFDM) [52].

2.7.1.4 Direct Detection Optical OFDM (DD-Optical OFDM)

The DD-Optical OFDM system block diagram includes a transmitter, a channel, and a receiver are depicted in Fig. 2.14. The transmitter creates the electrical OFDM signal that is transformed by a modulator into the optical domain by the electrical-optical (E / O) to the optical converter. The resulting optical signal is transmitted through the underwater channel. An optical to electrical (O / E) converter is utilized to convert the incoming optical signal to the electrical domain at the receiver which is considered in this case a photodiode [54]. The received electrical signal $A_e(t)$ is given by [55]:

$$A_e(t) = |A_o(t)|^2 \times h_e(t) + w(t) \qquad (2.15)$$

Where the $A_0(t)$ is optical OFDM signal, $h_e(t)$ is the impulse response in the electrical domain for the link, and $w(t)$ is the system noise. Then passes across a low-pass filter (LPF) after back-converting the signal, and is sent to the OFDM receiver for the initial signal.

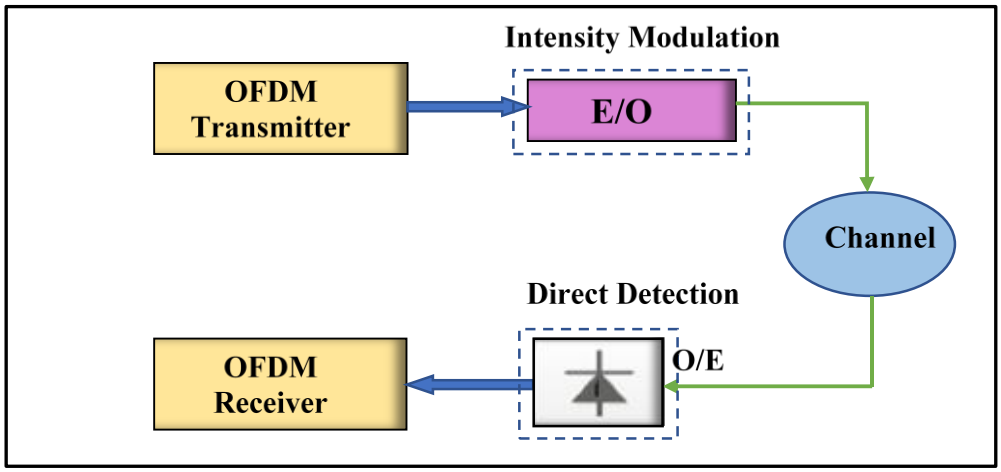

Fig. 2.14: DD-Optical OFDM System Block Diagram [55].

2.7.1.5 Coherent Detection Optical OFDM (CD-Optical OFDM)

Shieh and Athaudage were the first proposed of CD-Optical OFDM [54], it offers excellent performance in terms of spectral efficiency, receiver sensitivity , tolerance to chromatic and polarization dispersion and therefore offers greater system capacity-reach performance if compared with DD-Optical OFDM. However, this performance requires high transceiver complexity which results in higher cost compared to a DD-Optical OFDM. The schematic diagram of a typical CD-Optical OFDM system is depicted in Fig. 2.15; consisting of OFDM transmitter, RF-to-Optical Upconverter (RTO) unit, channel, Optical-to-RF downconverter (OTR) unit, and OFDM receiver [56]. CD-Optical OFDM employs modulation of the optical field therefore it can support complex time-domain signals both positive and negative frequency subcarriers can be used to carry data.

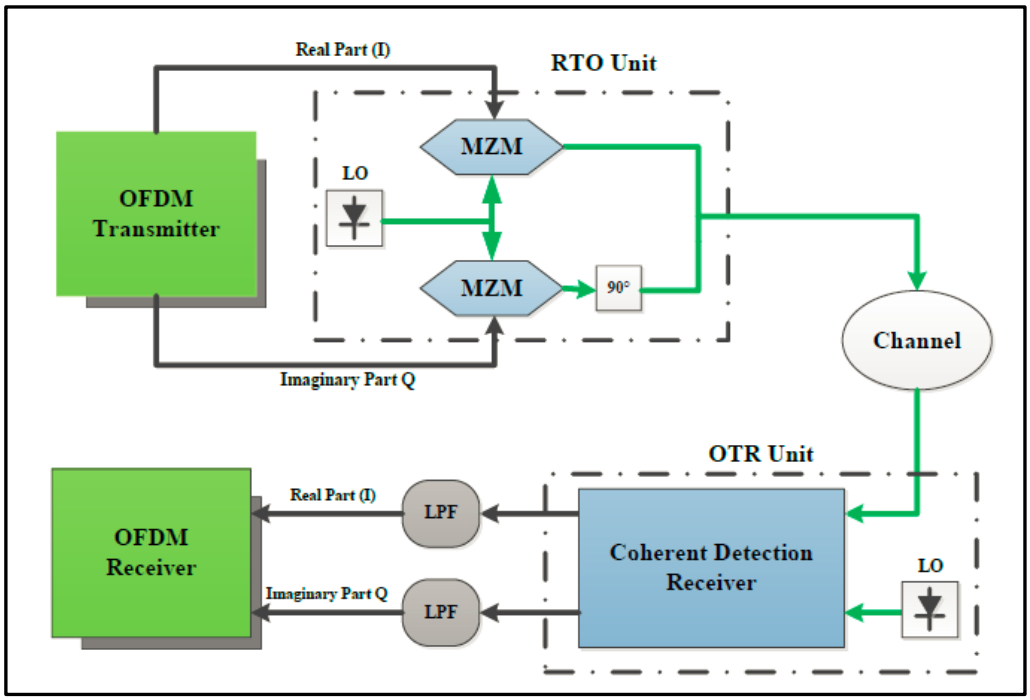

Fig. 2.15: CD-Optical OFDM System Block Diagram [54].

2.7.1.6 Optical-to-RF downconverter (OTR) Unit Architectures

The demodulation of an optical signal which needs phase, frequency, and polarization control requires a coherent detection receiver. To meet bandwidth growth demand and capacity, high order modulation formats and advanced multiplexing techniques are proposed. The coherent detection receivers are capable to detect various modulation formats. However, the direct detection receivers have a limited sensitivity as compared to the coherent detection receivers [45]. The coherent detection receivers were first used in the field of radio communications. This type of receiver is based on the coherence between the received signal phase and the Local Oscillator (LO) laser signal. To down-convert the received signal to the baseband, the received signal is mixed with the LO laser signal. There are many kinds of coherent detection receivers such us: single coherent receiver, single balanced coherent receiver, and balanced quadrature coherent receivers [45].

2.7.1.6.1 Single Coherent Receiver

The single coherent receiver is composed of a coupler (2×2), a local oscillator laser, and a single photodetector as illustrated in Fig. 2.16. The (2×2) coupler adds the detected signal together with the local oscillator signal in this receiver. A single photo-detector detects the total signal and for this reason it is called a single coherent receiver [52]. This receiver is unable to detect quadrature modulation formats. Thus, it is recommended for the detection of the OOK modulation format.

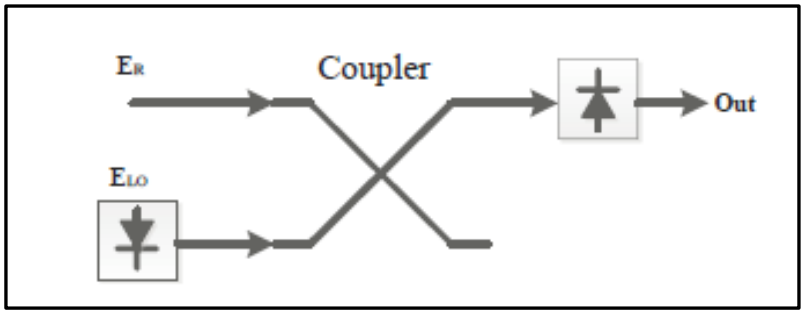

Fig. 2.16: Structure of Single Coherent Detection Receiver [51].

2.7.1.6.2 Balanced Coherent Receiver

The balanced coherent receiver is composed of LO laser, (2×2) coupler, and two balanced photodetectors, hence the name balanced coherent detection, as shown in Fig. 2.17. The two inputs of an optical coupler are fed by the received signal E_R and the local oscillator E_{LO} signal. For simplicity's sake, it is supposed that the received signal is only distorted by noise and not by channel dispersion [57].

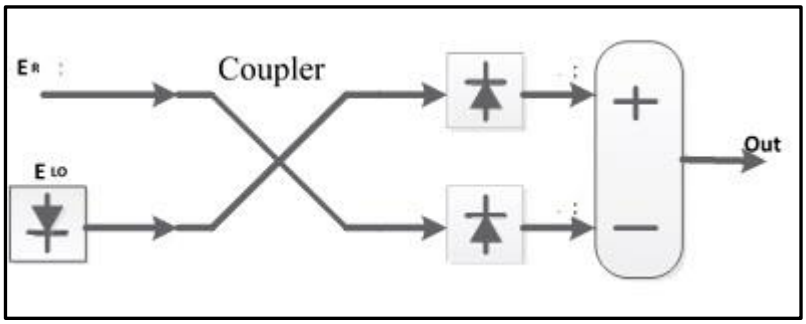

Fig. 2.17: Structure of Balanced Coherent Detection Receiver [57].

2.7.1.6.3 Balanced Quadrature Coherent Receiver

The balanced quadrature coherent receiver, as shown in Fig.2.18 is utilized to detect an optical received signal that is composed of an in-phase and quadrature components. In addition, this receiver can detect any optical modulation format [57]. The balanced quadrature coherent receivers convert the information about both the amplitude and the phase to the electrical domain. As shown in Fig. 2.18 in this receiver, the received signal with the local oscillator will be mixed by an optical 90° hybrid. Using two pairs of balanced photodetectors the total signal is detected. The 90° hybrid mixes the received signal and the LO signal to produce four quadrature states in complex-field space. The four signals are then fed into two pairs of balanced photodetectors [57].

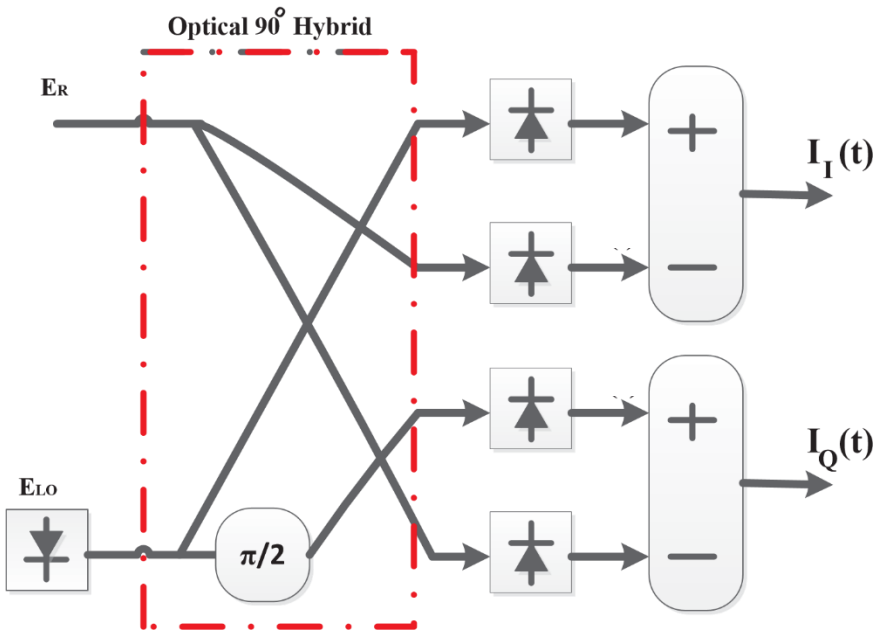

Fig. 2.18: Structure of balanced quadrature coherent detection receiver [57].

2.7.2 MIMO Techniques in Optical Communication

Because of the physical and chemical characteristics of water such as ocean surface and bottom reflection, temperature of sea, and ocean motion, the signal attenuation is great in the underwater communications. Thus, a technique which adapts to such an environment is motivated. MIMO has proven the atmospheric benefits of wireless communication. It will be a possible technology to utilize in the UOWC system. In fading channels, the MIMO system improves significantly channel capacity. This means that the transmission rate is significantly increased. In addition, the MIMO system also creates spatial diversity which reduces BER when the system is operated. The MIMO technique will combine the above-mentioned advantages of techniques to achieve reliable transmission for underwater wireless communication [49].

2.7.2.1 Mathematical Model of MIMO System

The model of MIMO system is illustrated in Fig. 2.19. The communication system consists of N_T transmitter elements and N_R receiver elements. Transmitter elements ($Tx_1 ....Tx_{NT}$) respectively send waves ($x_1, \ldots, x_{NT}$) to the receiver elements ($R_{x1}, \ldots, Rx_{NR}$). Every receiver element merges the incoming signals which coherently add up. The received waves at elements ($R_{x1}, \ldots, Rx_{NR}$) are respectively indicated by ($y_1, \ldots, y_{NR}$) as [58].

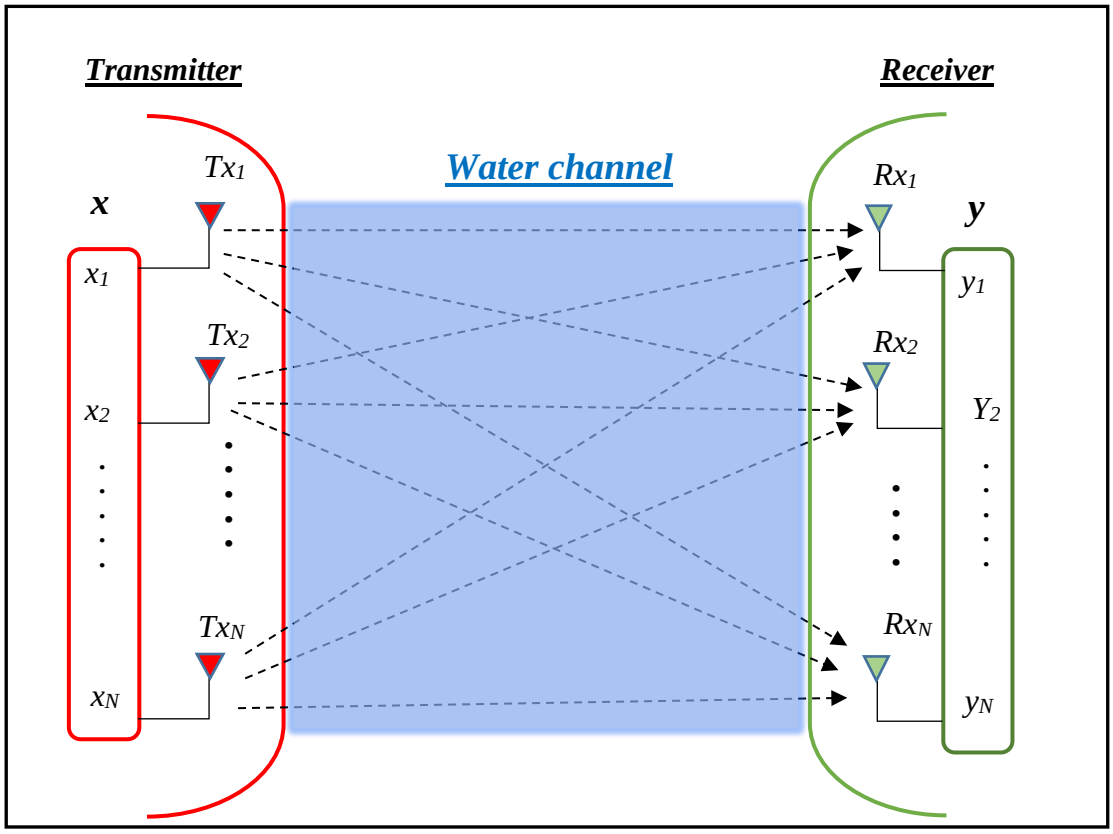

Fig. 2.19: MIMO System Model [58].

The received signal at elements Rx_q; q = 1, . . ., N_R

$$y_q = \sum_{p=1}^{N_T} h_{qp} \cdot x_p + b_q; q = 1,2,\ldots., N_R \qquad (2.16)$$

The input-output relationship describes the flat fading MIMO channel model [58]:

$$y = H \cdot x + b \tag{2.17}$$

where H is the ($N_R \times N_T$) complex channel matrix assumed by:

$$H = \begin{pmatrix} h_{11} & h_{12} & \dots & h_{1NT} \\ h_{21} & h_{22} & \dots & h_{2NT} \\ \vdots & \vdots & \ddots & \vdots \\ h_{NR1} & h_{NR2} & \dots & h_{NRNT} \end{pmatrix} \tag{2.18}$$

Where h_{qp} , $p = 1, \ldots, N_T$, $q = 1, \ldots, N_R$ is the complex channel gain which links transmitter elements Tx_p to receiver elements Rx_q.

- x = $[x_1, \ldots, x_{NT}]^T$ is the ($N_T \times 1$) complex transmitted signal vector.
- $Y = [y_1, \ldots, y_{NR}]^T$ is the ($N_R \times 1$) complex received signal vector .
- $b = [b_1, \ldots, b_{NR}]^T$ is the ($N_R \times 1$) complex additive noise signal vector.

CHAPTER THREE

SYSTEM DESIGN

3.1 Introduction

To give a correct design model of the UOWC system, suppose that we have a cluster or (layers structure) deployment of an Underwater Optical Wireless Sensor Network (UOWSN) starting from the ocean floor to the water surface. The first layer contain nodes or Sensors (S_s) which use data rate about 10Mbps where is not need a high data rate because they simply collect the environmental information such as (temperature, pressure …etc.), and it sends those data to the second layer above-called Cluster Head Level One (CH_{L1}) serve as relays, its function is to receive and forward data from the lower layer from (S_s) to the upper layer which called Cluster Head Level Tow (CH_{L2}) hop-by-hop to Surface Gateway (SG) and then to satellites, onshore, and inboard base-station, shown in Fig. 3.1 [59]:

Suppose we have many sensors equal to 1000 each one uses a data rate about 10 Mbps, each 100 S_S numbered (S_{S-1} - S_{S-100}) will be linked with one CH_{L1}, thus the summation of data rates at CH_{L1} will be about 1Gbps, suppose we have ten of CH_{L1} numbered (CH_{L1-1} - CH_{L1-10}) will be connected with one CH_{L2} the overall data rate will be 10 Gbps at CH_{L2} which will be delivered to the SG as shown in Fig. 3.1.

Depending on this structure, my design will be related to the transmission link between CH_{L2} and SG, which has a 10Gbps data rate and using the UOWC system.

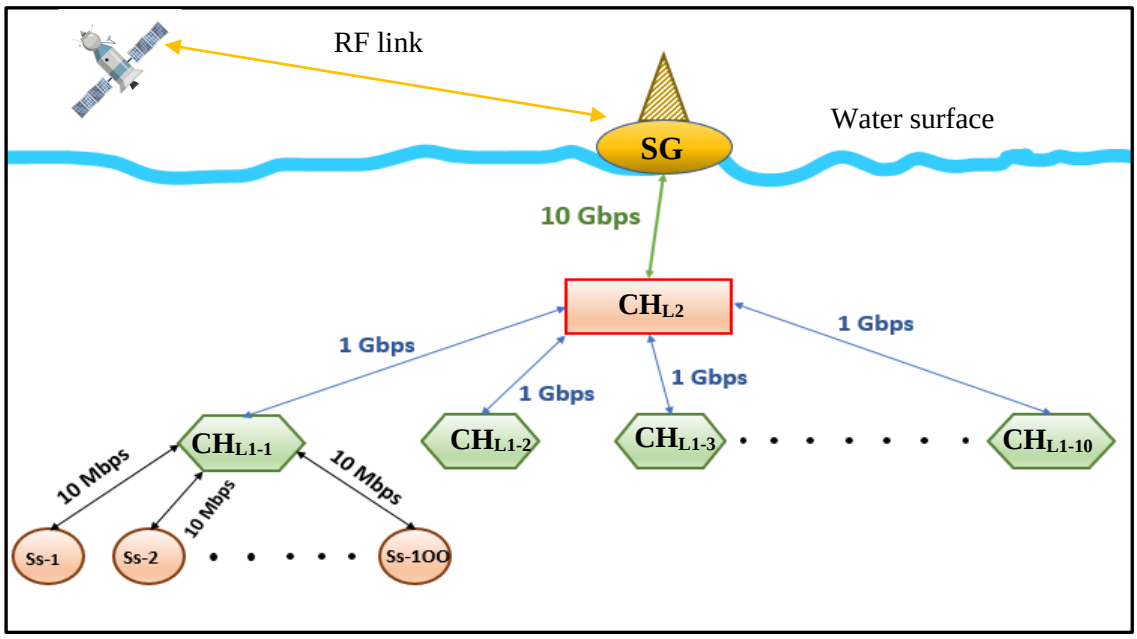

Fig 3.1: Clustering Structure of UOWSN and Used Data Rate for Each Link [59].

In this chapter, the information presented in the previous two chapters is used as a foundation for the design of the UOWC in the different water types. A brief description of OptiSystem software will be presented. Also, this chapter present, the system designs of the proposed UOWC as follows:

1. DPSK-DD-Optical OFDM with SISO.
2. DPSK-CD-Optical OFDM with SISO.
3. DPSK-DD-Optical OFDM and DPSK-CD-Optical OFDM with different MIMO configurations (1×2SIMO, 2×1MISO, 4×1SIMO, 4×1MOSO, 2×2MIMO, and 4×4MIMO respectively)

3.2 OptiSystem Software

Optisystem™ (Ver.16.0.0) from Optiwave Cooperation is an inclusive software design enabling users to design, test, and simulate optical links within the transmission layer of modern optical networks. This tool provides a huge number of optical and wireless components to plan and implement a

complete optical network, which is a time-saving, low-cost, and efficient method for the investigators. OptiSystem enables users to simulate and design the following: (1) Systems with multimode, (2) Access networks, (3) Co-Simulation with MATLAB program, (4) Analysis and design of fiber, (5) Optical code division multiple access for passive optical networks, (6) Advanced modulation, and finally (7) Optical receivers, transmitters, and amplifiers.

3.3 System Design of DPSK-DD-Optical OFDM with SISO

In Fig. 3.2 the DPSK-DD-Optical OFDM system is described. The system generally consists of several parts, i.e., an OFDM transmitter, an underwater channel, and OFDM receiver. The input data sequence length is set to 2^{15}-1 and it is built with a Pseudo-Random Bit Sequence (PRBS) generator are produced inside the BER Test Set unit, a bit sequence which is then applied into the 4DPSK sequence generator (encoder) to generate two parallel M-array symbol sequences from binary signals using differential phase shift keying modulation (DPSK). The M-Array sequence is transformed from serial to parallel form to blocks of information symbols; each may include 2 bits for M-array coding. These data symbols are converted into complex two-dimensional signals. The IFFT is used to generate the samples in the time domain. The DAC transforms the digital OFDM signal into analog form and eliminates the unwanted alias sideband signals by using a low-pass filter. The OFDM baseband signal is then transformed to an intermediate frequency (IF) signal via a quadrature modulator unit (IQ modulator), then to an optical domain, or converted directly to the optical domain according to device configuration. In phase (I) and quadrature (Q) of the resulting OFDM signal are transmitted parallel to overlap orthogonal subcarriers, whereby their (I) and (Q) electrical inputs are modulated with an RF carrier of 7.5 GHz by a quadrature modulator unit. The output RF signal is then fed to Intensity Modulation /Direct Detection (IM/DD). The electrical signal from the OFDM modulator will modulate by the MZM to the optical carrier with a LD of 450nm

(666.6 GHz center frequency). The LD has a power of 20dBm. The resulting optical signal from the Lithium Niobate Mach-Zehnder Modulator (LiNb-MZM) is then transmitted through the underwater channel. The opposite procedure is utilized at the receiver end to demodulate the original signal and recover it. The quadrate demodulator copies the electrostatic input signal, it is multiplied by sinusoidal and cosine carriers. The optical signal sent thought the optical link from a LD to a recipient is detected by a PIN detector with 1 A / W responsivity (which is a measure of input-output gain of the detector with unit A/W), 1×10^{-22} W / Hz thermal noise, 10nA dark current.

After converting the optical signal to an electrical signal and eliminating all the noise, the signal is going to be down-converted from 7.5 GHz RF carrier to the OFDM signal stage.

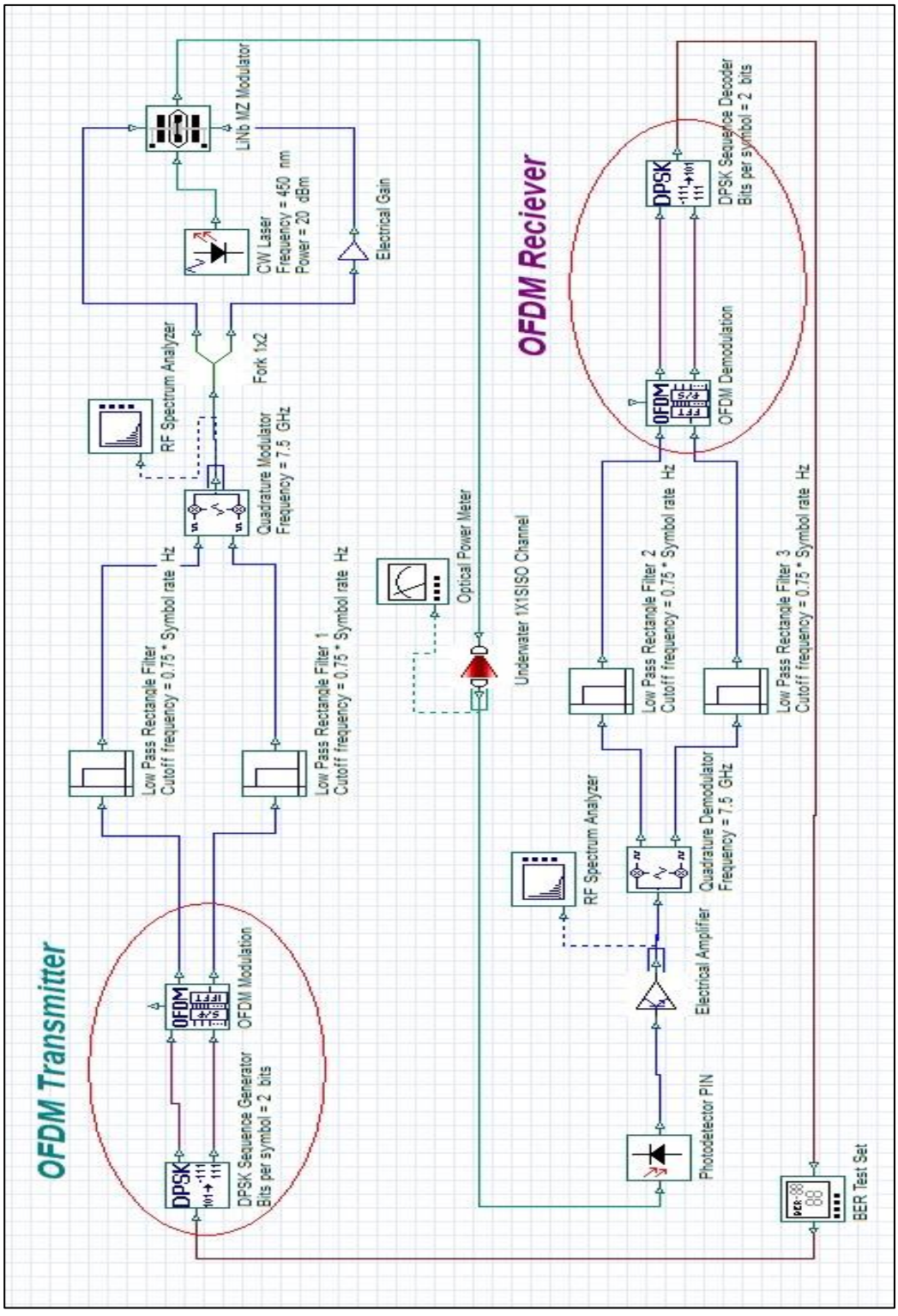

Fig. 3.2: System Design for the Proposed DPSK-DD-Optical OFDM System.

After filtering, the signal will be filtered by a low pass filter that removes the noise from signal, the filter will have an RF signal frequency. With each OFDM symbol, the OFDM demodulator eliminates the guard periods and then applies the FFT stage and regenerates the transmitted signal. The 4DPSK

sequence decoder decodes the two M-Array inputs into a one binary output, and the BER of the system is calculated by the BER Test Set unit. Table 3.1 shows the global parameter settings of the proposed DPSK-DD-Optical OFDM system.

Table-3.1: Main Parameters of the Proposed DPSK-DD-Optical OFDM System.

Parameter	Value	Note
Bit rate	10Gbps	High data rate [28]
Modulation	4DPSK	Low PAPR [60]
Symbol Rate	5 G S/s	each symbol contains 2 bits
Optical Transmitter (LD)	LD Wavelength=450nm	Low absorption and scattering [4]
	Transmitter Power=20dBm	Low power consumption [23]
	Transmitter aperture=50mm	Beam Divergence = 2mrad [61]
Optical Receiver Photo Detector (PIN)	Responsivity =1A/W [23]	High
	Dark current = 10 nA [61]	Low
	Thermal noise =$1x10^{-22}$ W/Hz [61]	Low
	Receiver aperture=75mm	
OFDM Subcarrier	1024 [50]	$N_{FFT/IFFT}$ = 2048 [52]
Channel	Water	Different types (clean, coastal and turbid) [4]
Sequence Length	2^{15}-1 =32767 bits	optional
Turbulence Model	Gamma-Gamma model [46]	weak to strong turbulence condition
Link Configuration	Line of Sight	The point-to-point underwater connection between transmitter and receiver [4].

3.4 System Design of DPSK-CD-Optical OFDM with SISO

In Fig. 3.3 the proposed DPSK-CD-Optical OFDM system is described. The system of DPSK-CD-Optical OFDM has the same architecture of DPSK-DD-Optical OFDM except two additional units, namely RF to optical unit (RTO) at the transmitter and optical to RF unit (OTR) which contains Coherent Detection (CD) at the receiver, as shown in Fig. 3.4 and Fig. 3.5. The input data sequence length is set to 2^{15}-1 and it is built with a Pseudo-Random Bit Sequence (PRBS) generator are produced inside the BER Test Set unit, a bit sequence which is then applied into the 4DPSK sequence generator (encoder) to generate two parallel M-array symbol sequences from binary signals using differential phase shift keying modulation (DPSK). The encoder's output is linked to an OFDM modulator with a number of subcarriers equal to 1024 at 2048 FFT points. The resulting signal from the OFDM modulator is then fed to quadrature modulator unit.

The in-phase (I) and quadrature (Q) are fed to the RTO upconverter unit. The RTO upconverter unit architecture is shown in Fig. 3.4. The RTO unit is made by utilizing a two X-coupler, two Mach-Zehnder modulators and an optical amplifier unit. In the output ports which will feed to the MZMs, the (I) and (Q) carry components are displayed as depicted in Fig. 3.4 on the 1st input port of the coupling coupler. The dual-drive Lithium Niobate Mach-Zehnder Modulator (LiNb-MZM) is used. At each MZM one of the basebands OFDM (I or Q) signal components at the two inputs of the MZM's modulation signal is supported by positive and negative signals. Both MZM 's output signals are merged into the complex optical OFDM signal to be amplified and transmitted using the optical combiner.

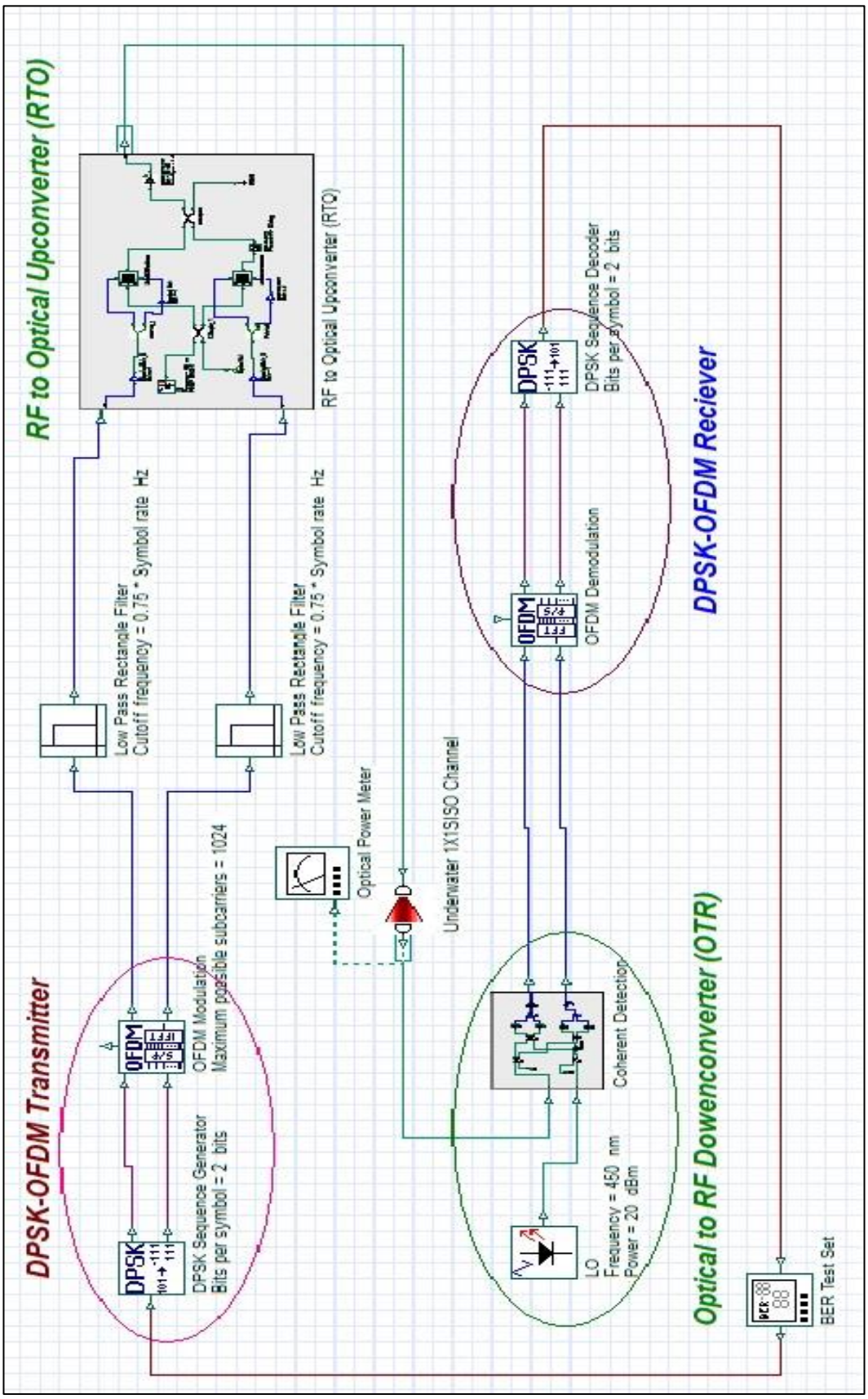

Fig. 3.3: System Design for the Proposed DPSK-CD-Optical OFDM System.

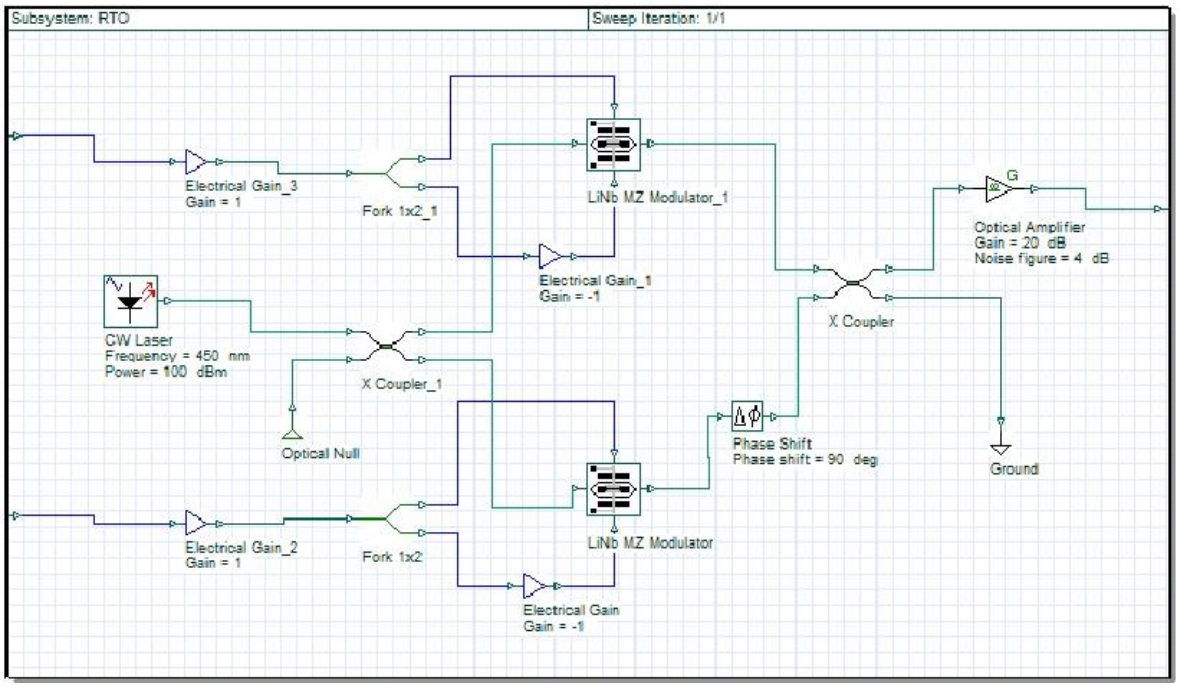

Fig. 3.4: Subsystem design for: RTO unit.

At the receiver, the Optical to RF downconverter (OTR) unit consist of four x-couplers, a 90^{o} phase shifter, PIN photodetectors with 1A/W responsivity (which is a measure of input-output gain of the detector with unit A/W), and two electrical subtractors, as depicted in Fig. 3.5. This OTR unit utilize balanced noise detectors. To separately extract the (I) and (Q) components in the OFDM, the first coupler splits the incoming optical OFDM complex signal into two parts. Likewise, the second coupler is utilized in the (I) and (Q) branches to split the LO signal into two sections to be combined with the Optical OFDM signal. At the third coupler, the LO signal in one of the branches is phase-shifted with 90^{o} by the optical phase shifter to be combined with the Optical OFDM signal. The outputs from the third coupler are required to be applied to the balanced detector PDs in order to produce the (I) component of the baseband OFDM signal after the output of the two PDs is subtracted, as illustrated in Fig. 3.5. Similarly, the (Q) component of the OFDM baseband signal is created in the balanced detector comprising the fourth coupler.

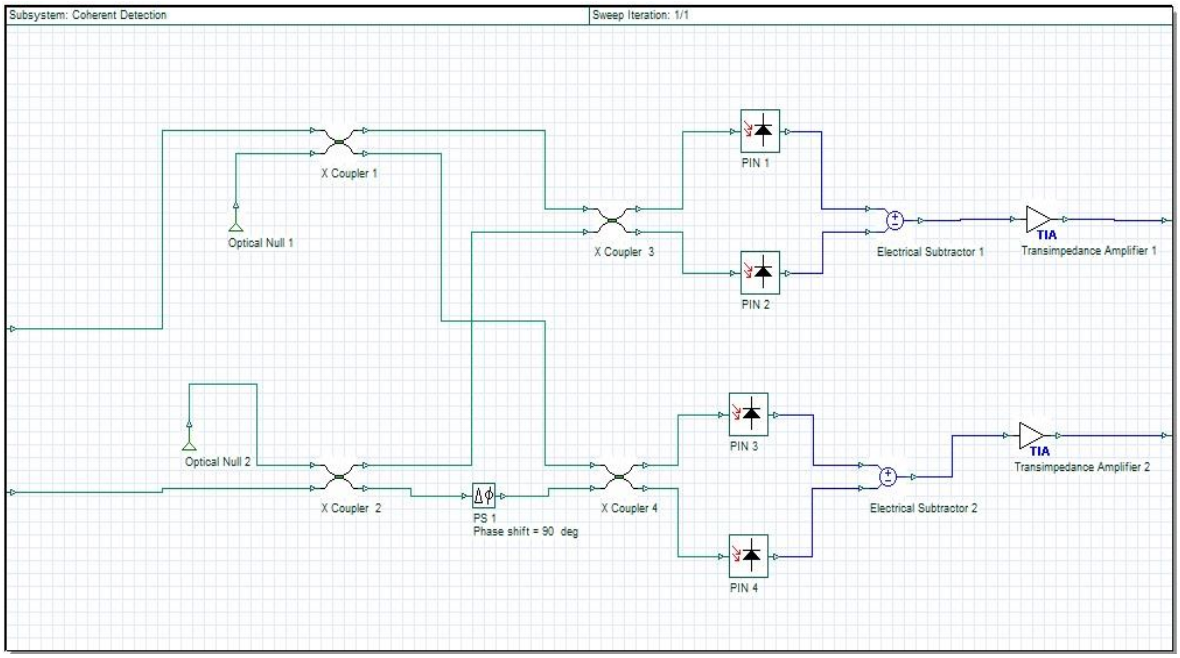

Fig. 3.5: Subsystem design for: Coherent Detection or OTR unit.

The output of the OTR unit is (I) and (Q) signal is then fed into the OFDM receiver, the OFDM receiver eliminates the guard periods and then applies the FFT stage and regenerates the transmitted signal. The 4DPSK sequence decoder decodes the two M-Array inputs into a one binary output, and the BER of the system is calculated by the BER Test Set unit. Table 3.2 illustrate the proposed DPSK-CD-Optical OFDM system main parameters.

Table-3.2: Main Parameters of the Proposed DPSK-CD-Optical OFDM System.

Parameter	Value	Note
Bit rate	10Gbps	High data rate [28]
Modulation	4DPSK	Low PAPR [60]
Symbol rate	5 G S/s	each symbol contains 2 bits
Optical Transmitter (LD)	LD Wavelength=450nm	Low absorption and scattering [4]

	Transmitter Power=20dBm	Low power consumption [23]
	Transmitter aperture=50mm	Beam Divergence = 2mrad [61]
Optical Receiver Photo Detector (PIN)	Responsivity =1A/W [23]	High
	Dark current = 10 nA [61]	Low
	Thermal noise =$1x10^{-22}$ W/Hz[61]	Low
	Receiver aperture=75mm	
OFDM Subcarrier	1024 [50]	$N_{FFT/IFFT}$ = 2048 [52]
Channel	Water	Different types (clean, coastal and turbid) [4]
Sequence length	2^{15}-1 =32767 bits	optional
Turbulence model	Gamma-Gamma model [46]	weak to strong turbulence condition
Coherent detection type	Balanced Quadrature Coherent Receiver	able to detect any optical modulation format [57]
Link Configuration	Line of Sight	The point-to-point underwater connection between transmitter and receiver [4].

3.5 System Design of DPSK-DD-Optical OFDM and DPSK-CD-Optical OFDM with different MIMO Configurations

To improve UOWC system performance and make it capable to communicate and sense at the same time, the MIMO technique is proposed. MIMO technique has been introduced into UOWC systems with the advantages of performance enhancement compared with the SISO technique.

In this thesis, the DPSK-DD-Optical OFDM is based on different proposed MIMO configurations depicted in Fig. 3.6 and the DPSK-CD-Optical OFDM based on different proposed MIMO configurations are depicted in Fig. 3.7.

These designs are the same architecture in the previous sections 3.3 and 3.4 excepting using the MIMO subsystem component.

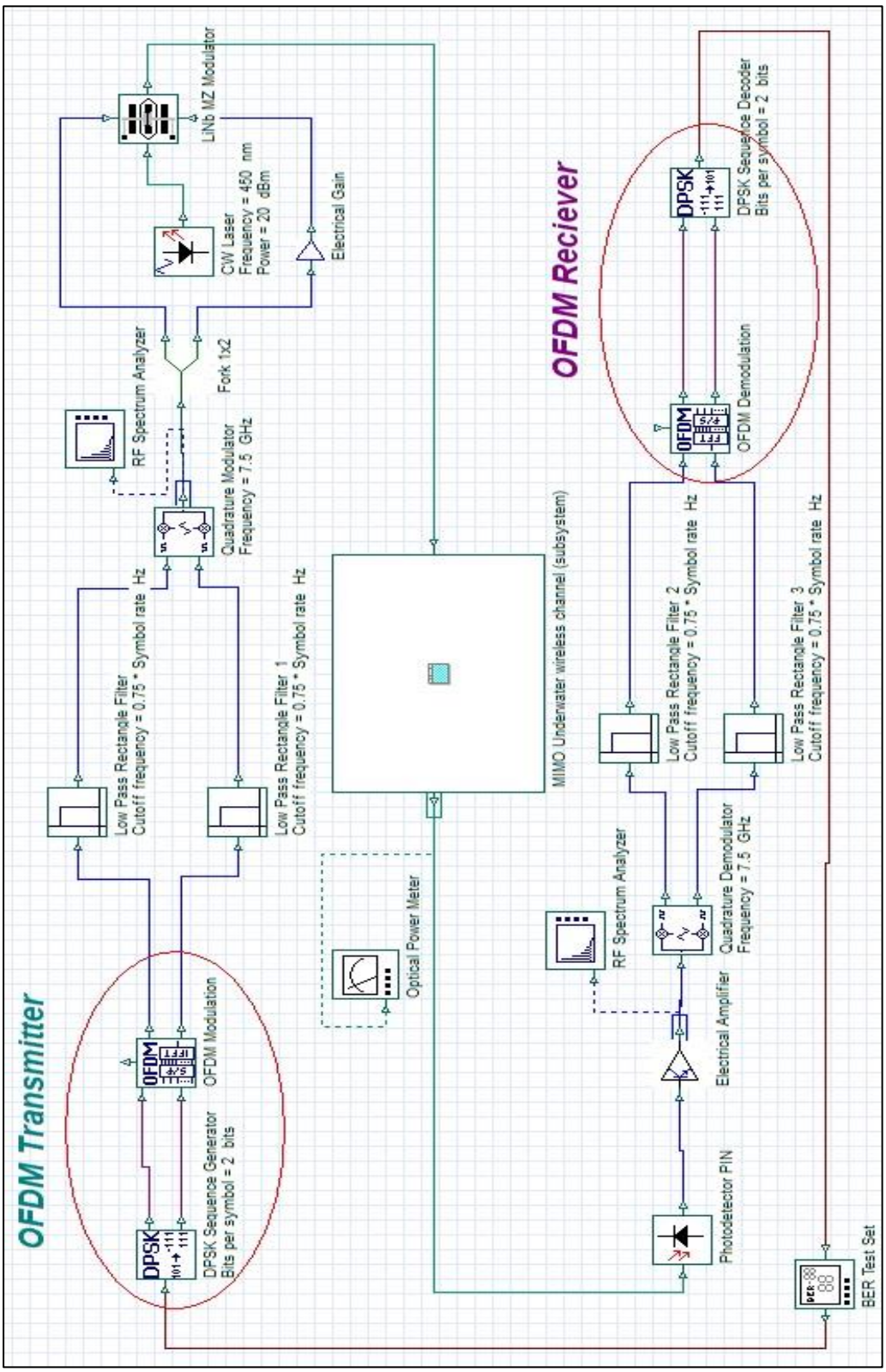

Fig. 3.6: System design of DPSK-DD-Optical OFDM with MIMO subsystem.

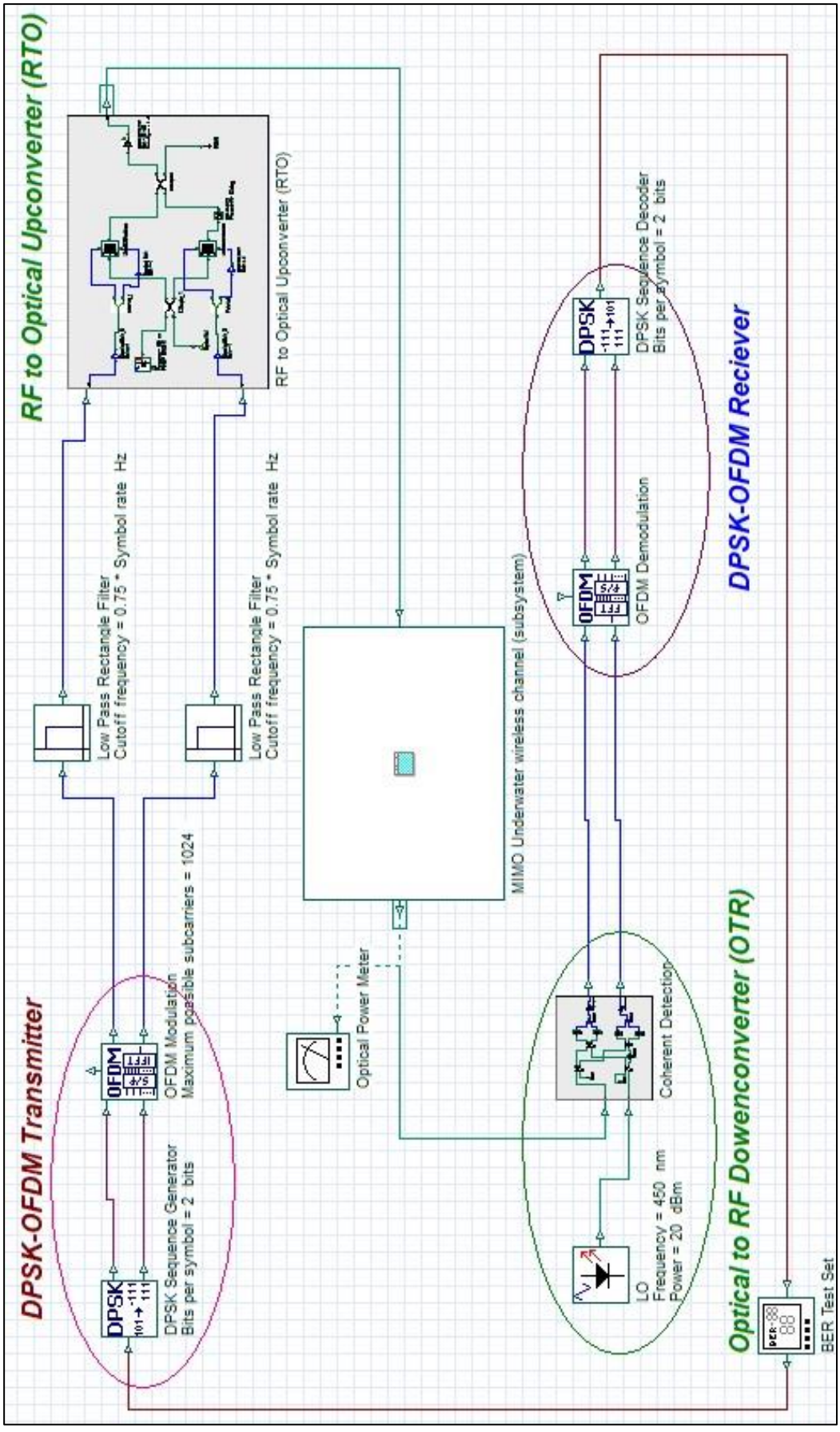

Fig. 3.7: System design of DPSK-CD-Optical OFDM with MIMO subsystem.

In UOWC system design the MIMO subsystem represents different MIMO configurations (*1×2SIMO, 2×1MISO, 4×1SIMO, 4×1MOSO, 2×2MIMO, and 4×4MIMO* respectively) as shown in Fig. 3.8 (a-f). All different MIMO configurations architecture comprise of a number of power combiner, power splitter, fork, and underwater channel depending on MIMO configurations.

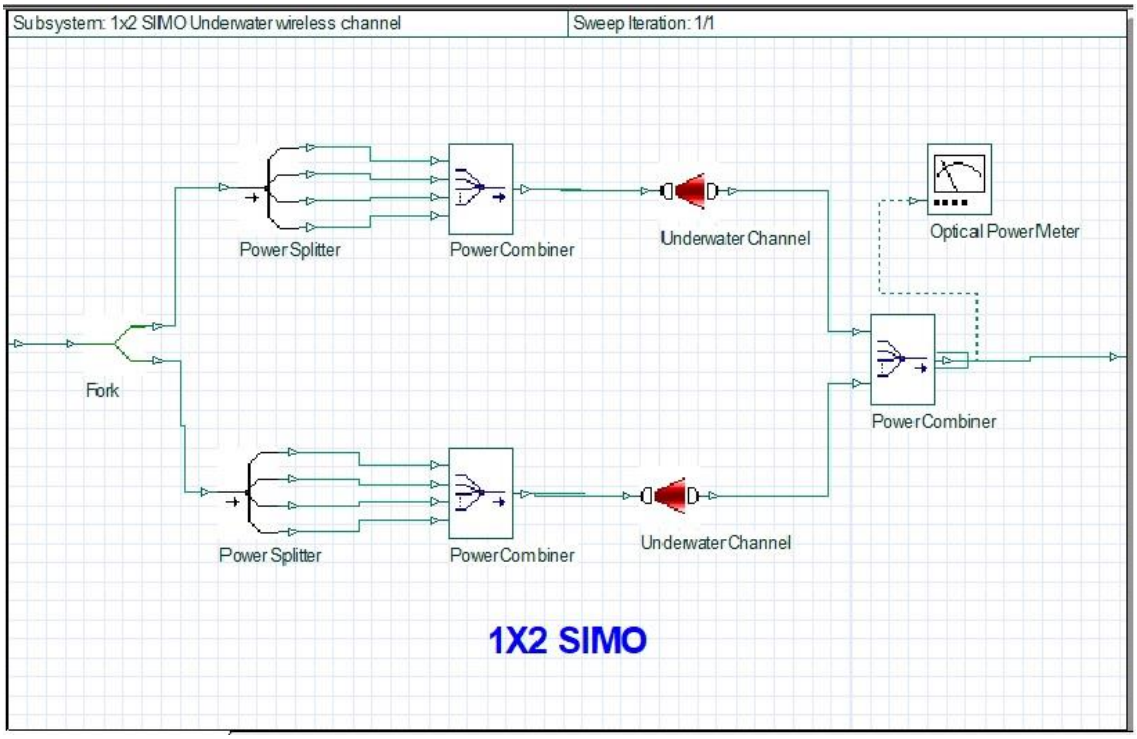

(a)

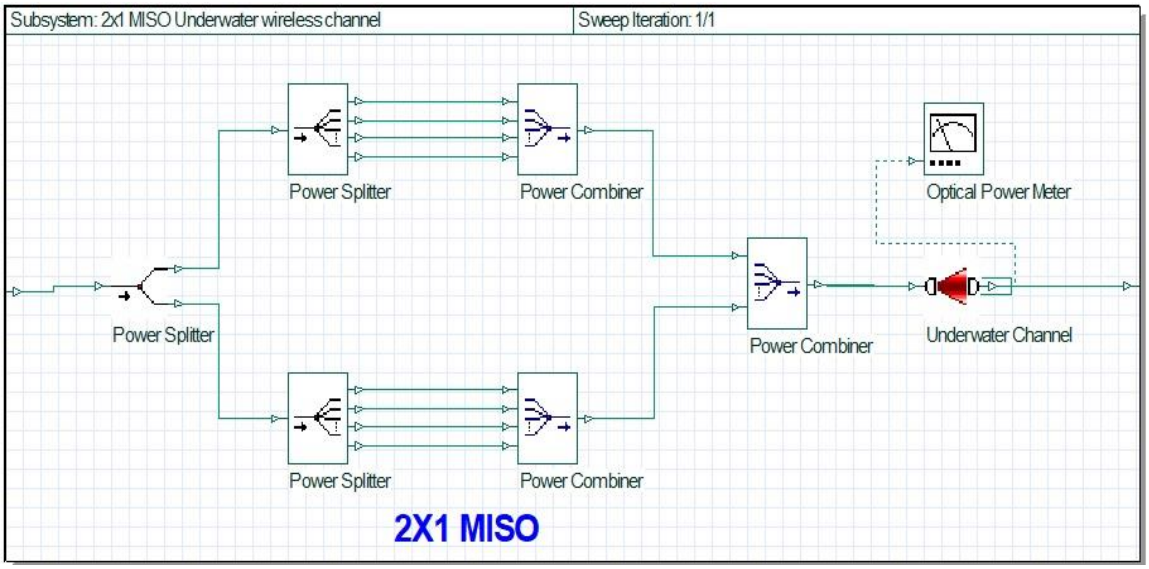

(b)

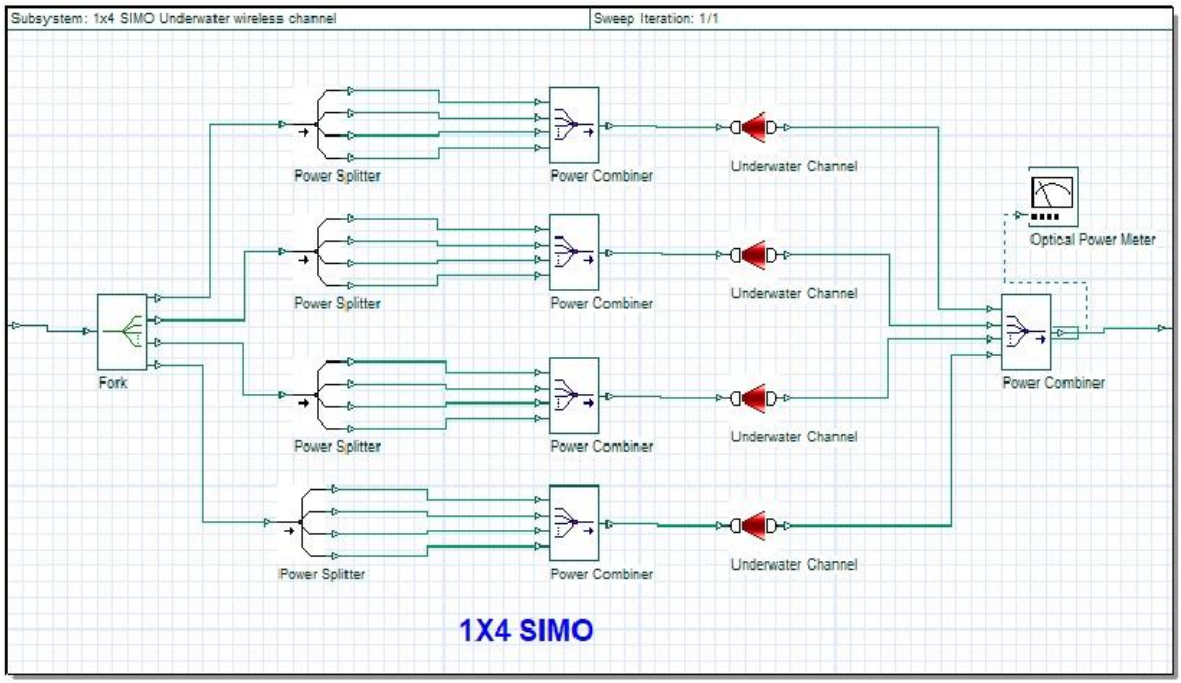
Subsystem: 1x4 SIMO Underwater wireless channel
Sweep Iteration: 1/1
Power Splitter
Power Combiner
Underwater Channel
Optical Power Meter
Fork
1X4 SIMO

(c)

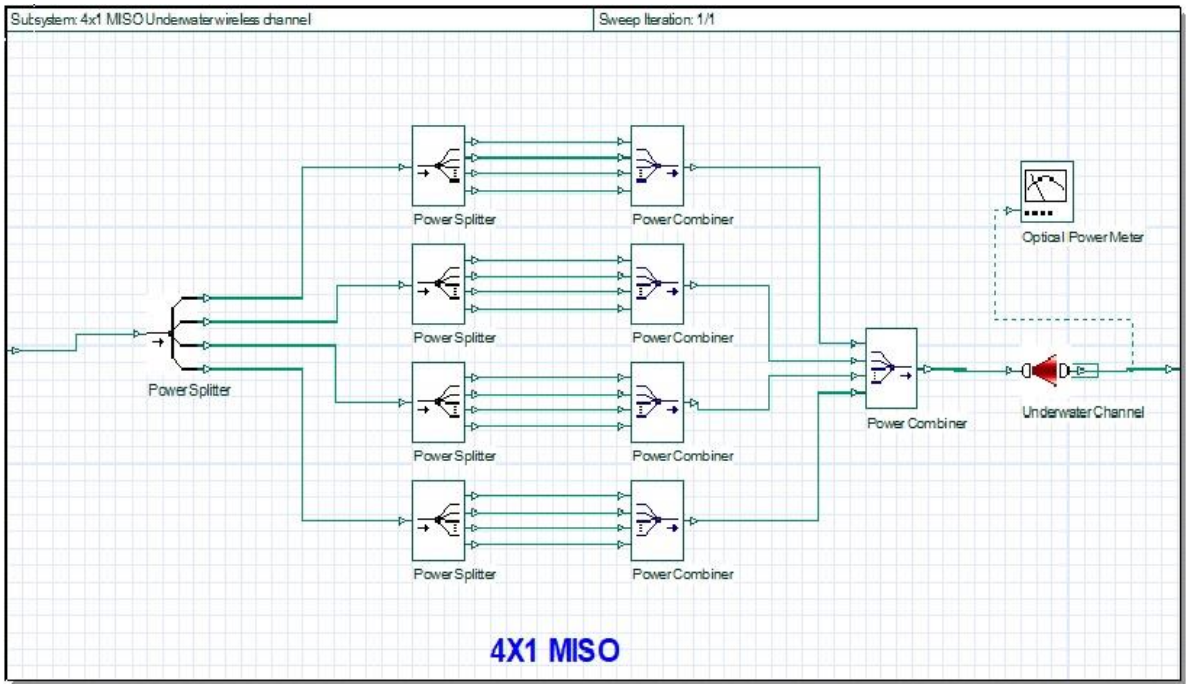
Subsystem: 4x1 MISO Underwater wireless channel
Sweep Iteration: 1/1
Power Splitter
Power Combiner
Optical Power Meter
Underwater Channel
4X1 MISO

(d)

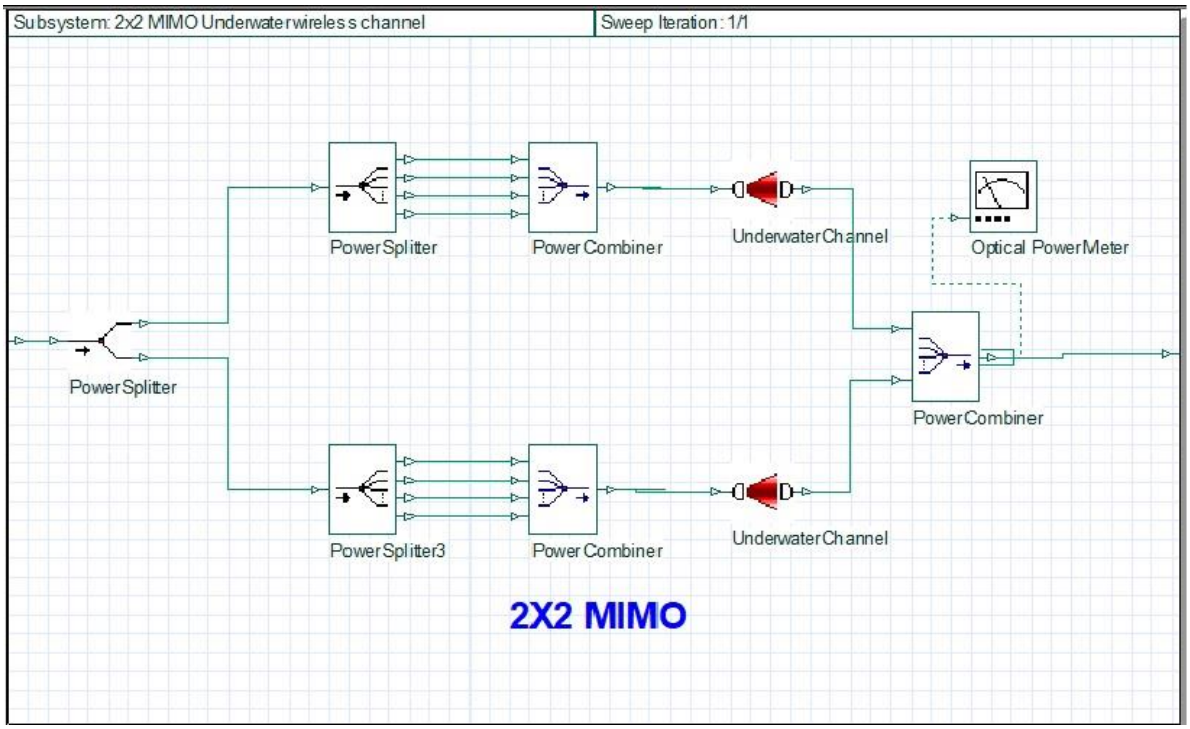

(e)

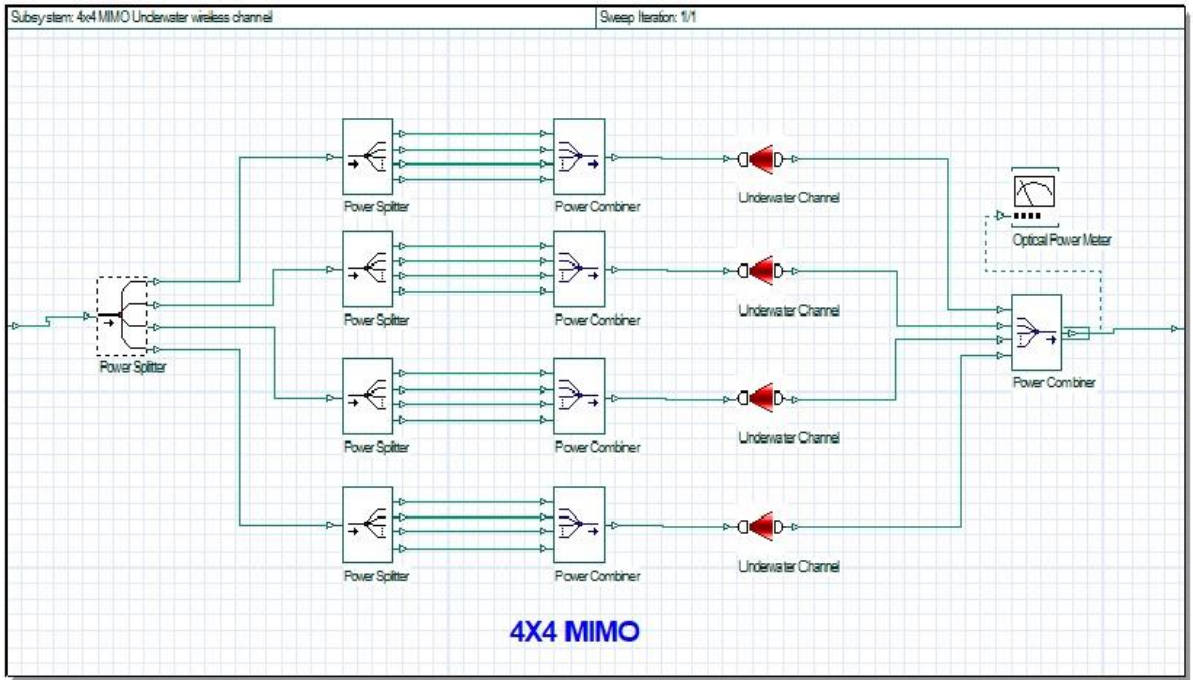

(f)

Fig. 3.8: MIMO Subsystem Design of (a) 1×2SIMO, (b) 2×1MISO, (c) 1×4SIMO, (d) 4×1MISO (e) 2×2MIMO and (f) 4×4MIMO.

CHAPTER FOUR

SIMULATION RESULTS AND ANALYSIS

4.1 Introduction

In this chapter, a UOWC system is simulated and analyzed by incorporating commercial software Optisystem^{TM}. The performance of the UOWC system is studied within various types of water and link ranges. The main modulation format DPSK is used in the simulation. This modulation is strong against water turbulence, weak signals, and give low PAPR. Also, the performance evaluation of the suggested DPSK-DD-Optical OFDM with the SISO and different MIMO configurations are investigated in the different distances and water types, to identify the key role played by the MIMO technique. The investigation is then expanded to include the DPSK-CD-Optical OFDM technique incorporating various MIMO configurations in the different distances and water types.

The end-to-end BER of the suggested DPSK-DD-Optical OFDM, DPSK-CD-Optical OFDM based on 1×1SISO, and various MIMO configurations are calculated under different distances and water types. The results analysis also compares the BERs between proposed DPSK-DD-Optical OFDM with MIMO and DPSK-CD-Optical OFDM with the MIMO system. Also, the received power will be presented and discussed.

4.2 Simulation Results of DPSK-DD-Optical OFDM with SISO and Different MIMO Configurations

The BER performances of the proposed DPSK-DD-Optical OFDM are studied under various transmission lengths and three water types (clear, coastal, turbid).

In clear water (low turbulence channel) the numerical results of BER_s which have been obtained are 3.8×10^{-5} at 52m using 1×1SISO, 5.3×10^{-5} at 95m using 1×2SIMO, 1.5×10^{-5} at 114m using 1×4SIMO, 8.2×10^{-5} at 72m using 2×1MISO, 4.2×10^{-5} at 64m using 4×1MISO, 2×10^{-5} at 101m using 2×2MIMO and 2.46×10^{-5} at 131m using 4×4MIMO respectively.

Figure 4.1 displays the diagram of BER versus link range of DPSK-DD-Optical OFDM with 1×1SISO and different MIMO configurations (1×4SIMO, 1×2SIMO, 2×1MISO, 4×1MISO, 2×2MIMO and 4×4MIMO respectively) under clear water (low turbulence channel).

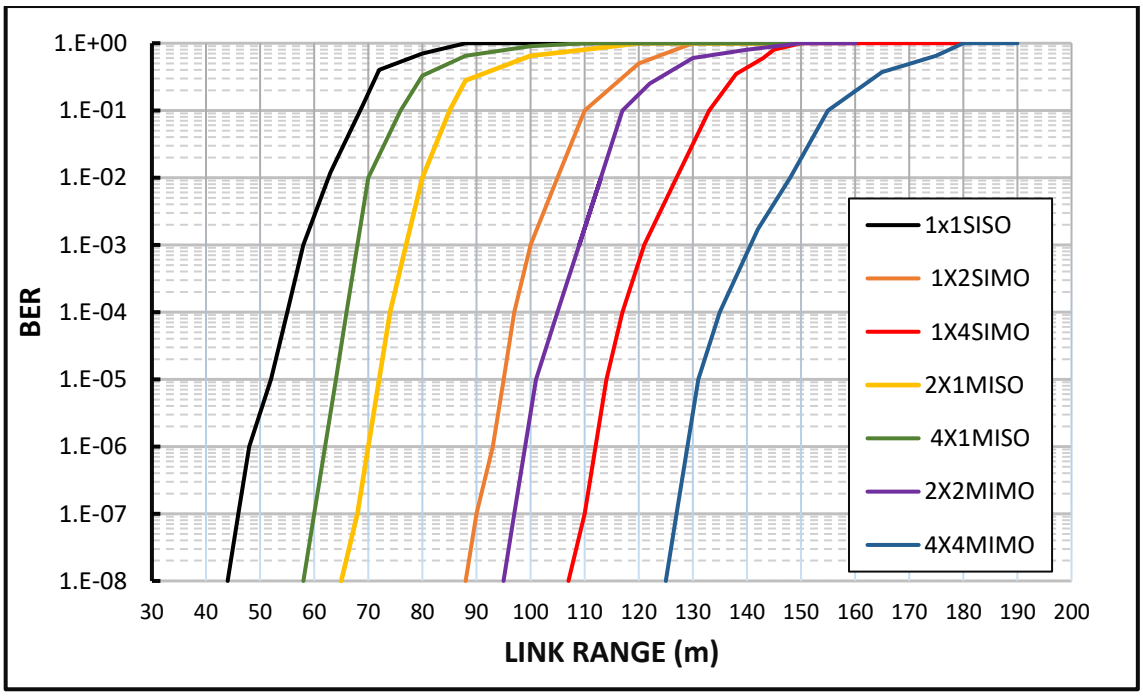

Fig. 4.1: BER vs. Link Range for DPSK-DD-Optical OFDM with various MIMO configurations under clear water (Low Turbulence Channel).

In mid (coastal) water the numerical results of BER_s which have been obtained are 5.9×10^{-5} at 21.3m using 1×1SISO, 4.7×10^{-5} at 25.15m using 1×2SIMO, 8.2×10^{-5} at 28.45m using 1×4SIMO, 9.1×10^{-5} at 23.95m using 2×1MISO, 2.2×10^{-5} at 22.7 using 4×1MISO, 3.6×10^{-5} at 26.1m using 2×2MIMO and 3.5×10^{-5} at 31m using 4×4MIMO respectively.

Figure 4.2 depicts the schematic graphic of BER versus the link range of DPSK-DD- Optical OFDM with 1×1SISO and different MIMO configurations (1×4SIMO, 1×2SIMO, 2×1MISO, 4×1MISO, 2×2MIMO and 4×4MIMO respectively) in coastal water (mid turbulence channel).

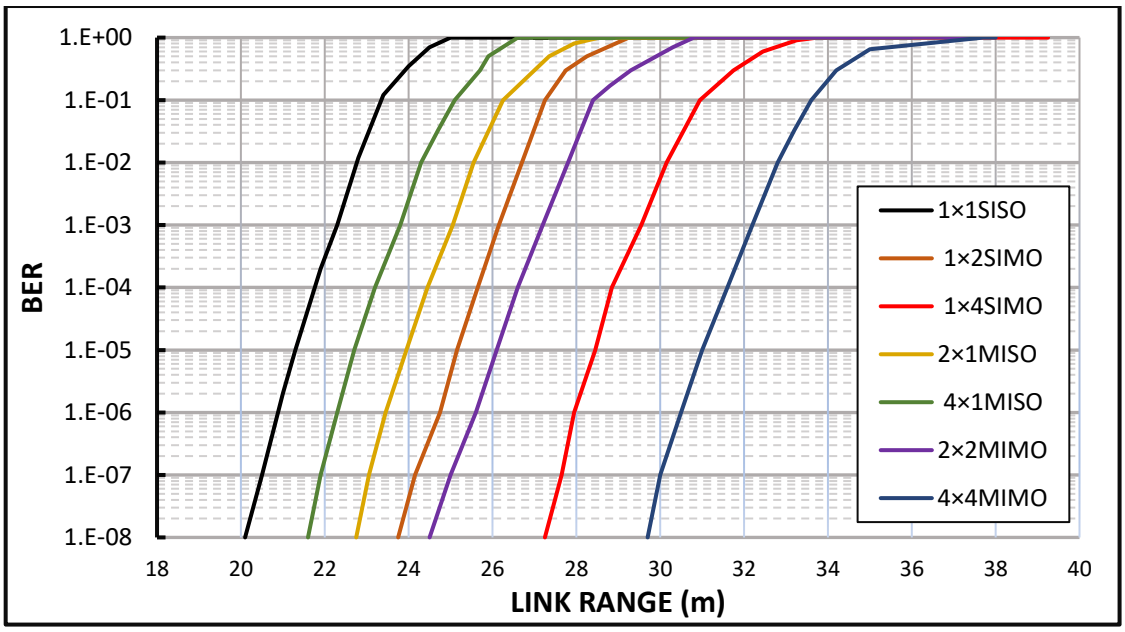

Fig. 4.2: BER vs. Link Range for DPSK-DD-Optical OFDM with various MIMO configurations under coastal water (Mid Turbulence Channel).

In turbid water (high turbulence channel) the numerical results of BER_s which have been acquired are 2.8×10^{-5} at 2.4m using 1×1SISO, 8.2×10^{-5} at 6.68m using 1×2SIMO, 7.3×10^{-5} at 8.45m using 1×4SIMO, 5.6×10^{-5} at 5m using 2×1MISO, 6.2×10^{-5} at 3.59m using 4×1MISO, 5.3×10^{-5} at 7.8m using 2×2MIMO and 3.9×10^{-5} at 10.5m using 4×4MIMO respectively.

Figure 4.3 depicts the schematic graphic of BER versus the link range of DPSK–DD-Optical OFDM with 1×1SISO and different MIMO configurations (1×4SIMO, 1×2SIMO, 2×1MISO, 4×1MISO, 2×2MIMO and 4×4MIMO respectively) in turbid water (high turbulence channel).

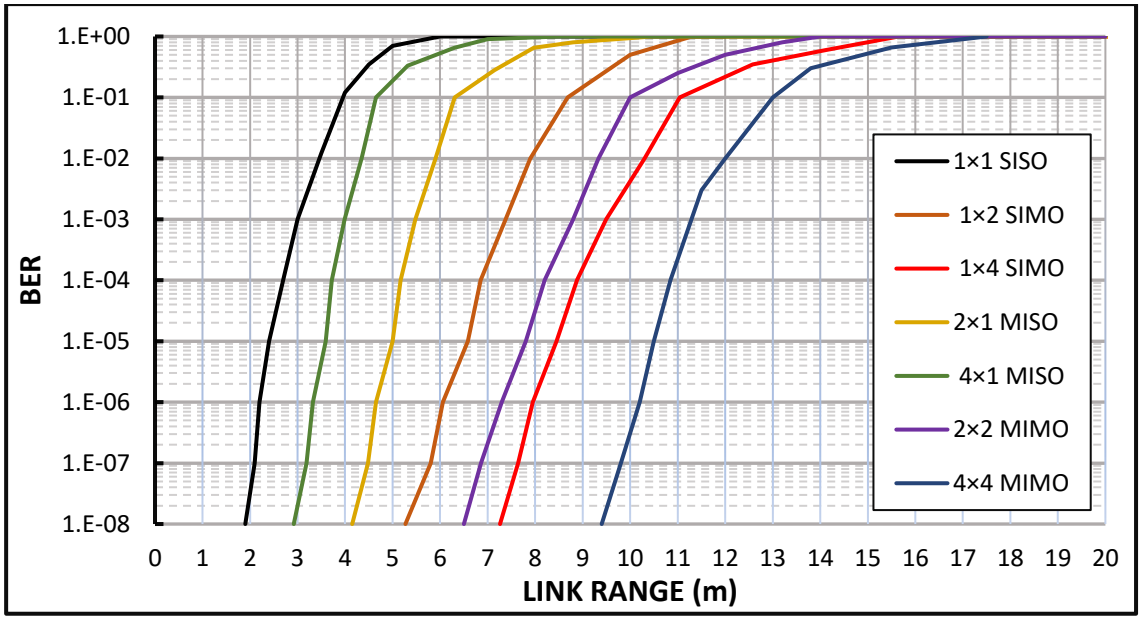

Fig. 4.3: BER vs. Link Range for DPSK-DD-Optical OFDM with various MIMO configurations under turbid water (High Turbulence Channel)

From the previous figures 4.1, 4.2, and 4.3, it is clear that the performance of 4×4MIMO and 1×4SIMO systems under three types of water (clear, coastal, turbid) are better than the other configurations (1×1SISO, 1×2SIMO, 2×1MISO, 4×1MISO and 2×2MIMO respectively). So, it is observed that the link range increased by increasing the receiver elements (photodetectors) at the objective BER which was equivalent to 10^{-5}.

The following figure 4.4 shows the diagram of the received power in (dBm) versus link range in (m) for DPSK-DD-Optical OFDM under three water types (clear water, coastal water, and turbid water respectively). It is worth noticing that

for any of the illustrated distances the transmitted power is constant and equal to 20dBm.

Figure 4.4 depicts the total power received at target BER for DPSK-DD-Optical OFDM with SISO are -11.68dBm at 52m under clear water, -2dBm at 21.3m under mid (coastal) water, and -9.2dBm at 2.4m under turbid water respectively.

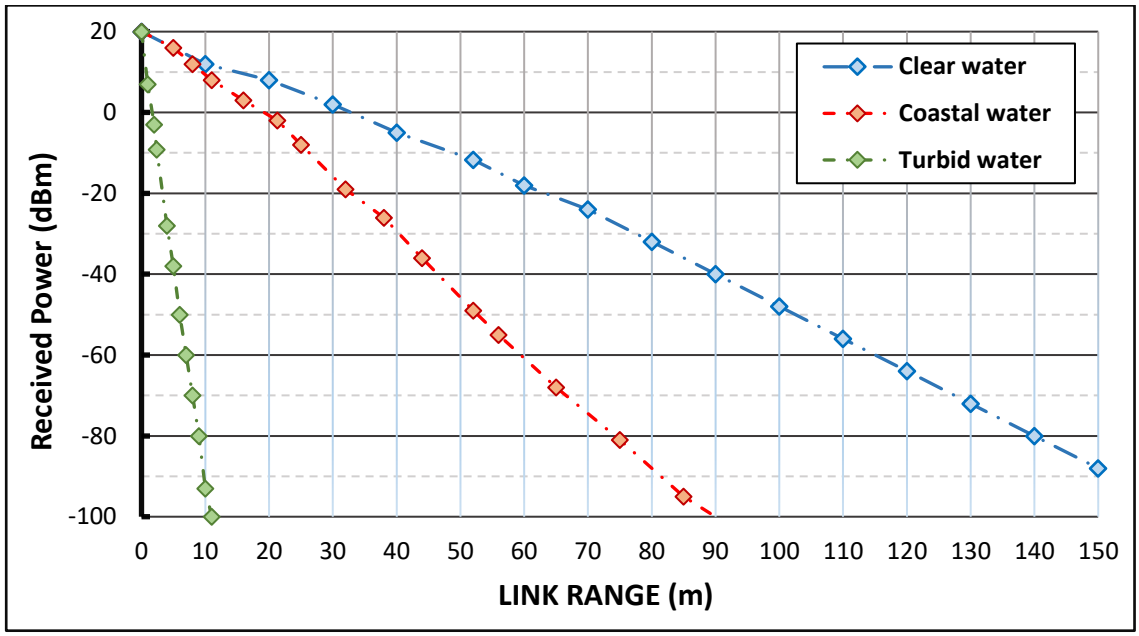

Fig. 4.4: Received Power (dBm) vs. Link Range (m) of DPSK-DD-Optical OFDM with SISO under three water types (clear water, coastal water, and turbid water).

From the above figure, it is quite obvious that the received power is linearly and inversely proportional to the link range.

4.3 Simulation Results of DPSK-CD-Optical OFDM with SISO and Different MIMO Configurations

The BER performances of the proposed DPSK-CD-Optical OFDM are studied under various transmission lengths and three water types (clear, coastal, turbid).

In clear water (low turbulence channel) the numerical results of BER_s which have been obtained are 2.3×10^{-5} at 71m using 1✕1SISO, 6.2×10^{-5} at 114m using 1✕2SIMO, 8.5×10^{-5} at 133m using 1✕4SIMO, 7.2×10^{-5} at 96m using 2✕1MISO, 2×10^{-5} at 83m using 4✕1MISO, 5.1×10^{-5} at 120m using 2✕2MIMO and 3.5×10^{-5} at 156m using 4✕4MIMO respectively.

Figure 4.5 displays the diagram of BER versus the link range of DPSK-CD - Optical OFDM with 1✕1SISO and different MIMO configurations (1✕4SIMO, 1✕2SIMO, 2✕1MISO, 4✕1MISO, 2✕2MIMO and 4✕4MIMO respectively) under clear water (low turbulence channel).

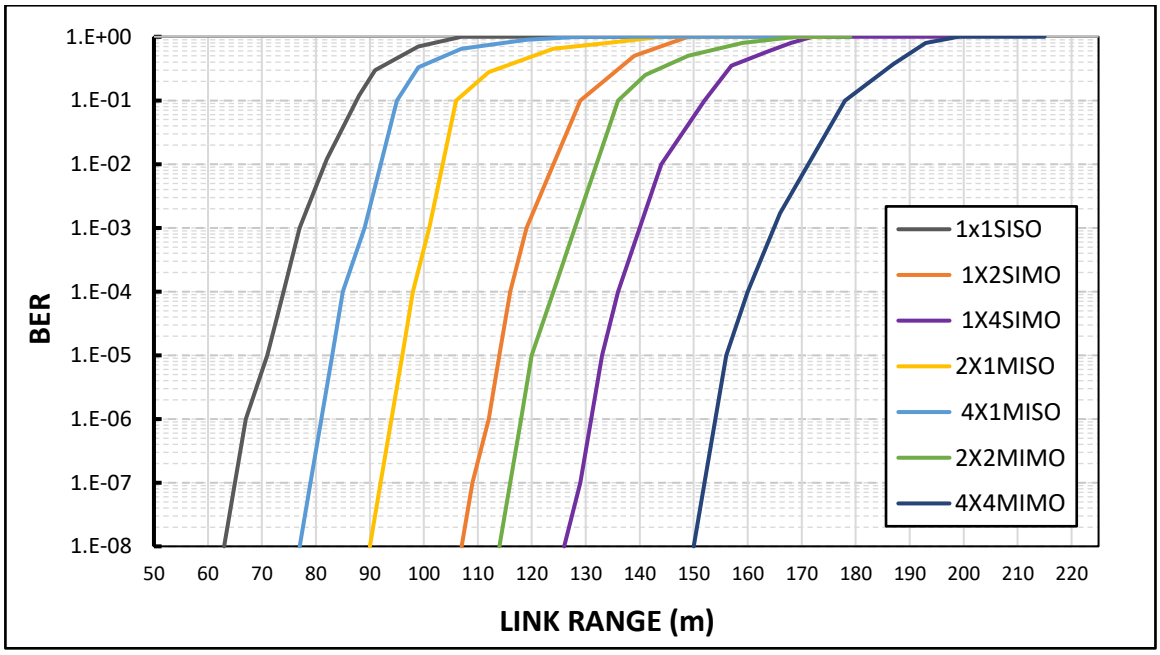

Fig. 4.5: BER vs. Link Range for DPSK-CD-Optical OFDM with various MIMO configurations under clear water (Low Turbulence Channel).

In coastal water (mid turbulence channel) the numerical results of BER_s which have been obtained are 4.7×10^{-5} at 29.8m using 1✕1SISO, 2.2×10^{-5} at 34.9m using 1✕2SIMO, 4.1×10^{-5} at 37.2m using 1✕4SIMO, 6.7×10^{-5} at 33.2m using 2✕1MISO, 4.2×10^{-5} at 31.7m using 4✕1MISO, 1.6×10^{-5} at 36.1m using 2✕2MIMO and 4.4×10^{-5} at 38.5m using 4✕4MIMO respectively.

Figure 4.6 depicts the schematic diagram of BER versus the link range of DPSK-CD-Optical OFDM with different MIMO configurations (1✕1SISO, 1✕4SIMO, 1✕2SIMO, 2✕1MISO, 4✕1MISO, 2✕2MIMO and 4✕4MIMO respectively) in coastal water (mid turbulence channel).

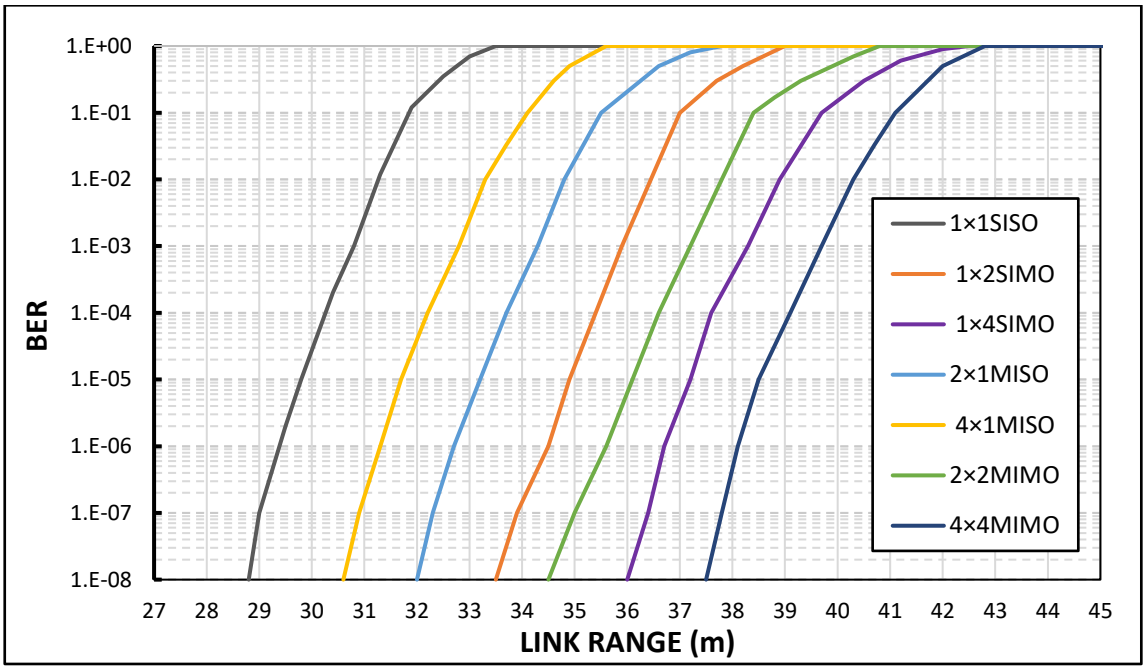

Fig. 4.6: BER vs. Link Range for DPSK-CD-Optical OFDM with various MIMO configurations under coastal water (Mid Turbulence Channel).

In turbid water (high turbulence channel) the numerical results of BER_s which have been acquired are 1.8×10^{-5} at 4.4m using 1✕1SISO, 4.3×10^{-5} at 8.58m using 1✕2SIMO, 7.2×10^{-5} at 10.2m using 1✕4SIMO, 6.2×10^{-5} at 7.5m using 2✕1MISO, 3.1×10^{-5} at 5.59m using 4✕1MISO, 4.3×10^{-5} at 9.3m using 2✕2MIMO and 2×10^{-5} at 12m using 4✕4MIMO respectively.

Figure 4.7 depicts the schematic diagram of BER versus the link range of DPSK-CD- Optical OFDM with different MIMO configurations (1×1SISO, 1×4SIMO, 1×2SIMO, 2×1MISO, 4×1MISO, 2×2MIMO and 4×4MIMO respectively) in turbid water (high turbulence channel).

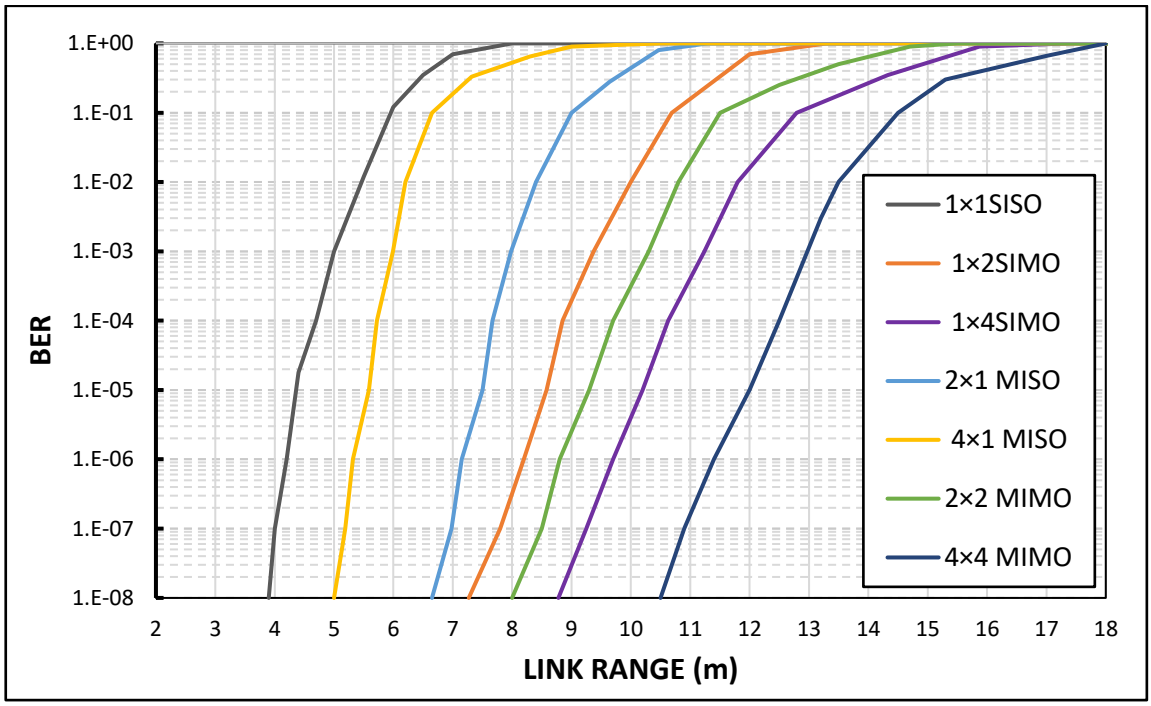

Fig. 4 7: BER vs. Link Range for DPSK-CD-Optical OFDM with various MIMO configurations under turbid water (High Turbulence Channel).

From the previous figures 4.5,4.6 and 4.7, the performance of 4×4MIMO and 1×4SIMO systems under three types of water are better than the other configurations (1×1SISO, 1×2SIMO, 2×1MISO, 4×1MISO and 2×2MIMO respectively). Using spatial diversity is one of the best techniques to mitigate or remove the turbulence effect. So, it is observed that the link range increased by increasing the receiver elements (photodetectors).

Because of increasing the receiver sensitivity to frequency and phase noise, the simulation results show the performance of overall DPSK-CD-Optical OFDM with a MIMO based system is better than DPSK-DD-Optical OFDM with a MIMO based system.

The following figure 4.8 shows the diagram of the received power in (dBm) versus link range in (m) for DPSK-CD-Optical OFDM under three water types (clear water, coastal water, and turbid water respectively). It is worth noticing that for any of the illustrated distances the transmitted power is constant and equal to 20dBm.

Figure 4.8 depicts the total power received for target BER for DPSK-CD-Optical OFDM with SISO is -28 dBm at 71m under clear water, -21dBm at 29.8m under mid (coastal) water, and -29.5dBm at 4.4m under turbid water respectively.

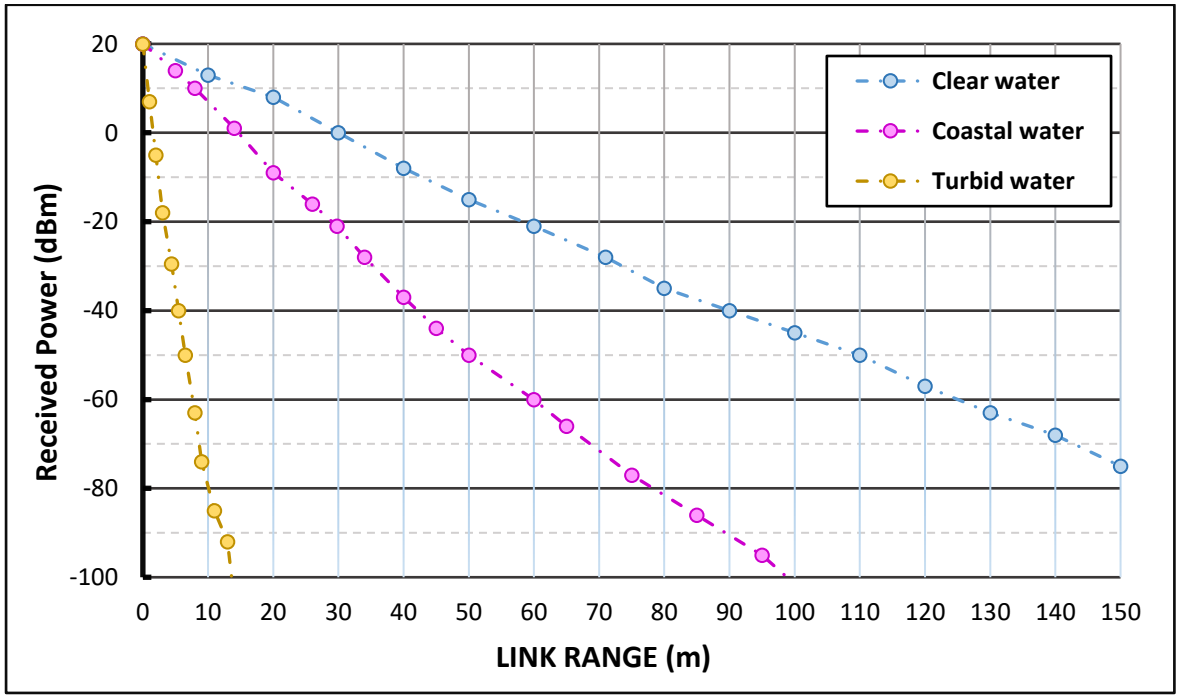

Fig. 4.8: Received Power (dBm) vs. Link Range (m) of DPSK-CD-Optical OFDM with SISO under three water types (clear water, coastal water, and turbid water).

From the above figure, it is quite obvious that the received power is linearly and inversely proportional to the link range.

4.4 The Summarization and Comparison of Results

The summarization of results comparison of DPSK-DD-Optical OFDM and DPSK-CD-Optical OFDM based on 1×1SISO and 4×4MIMO systems in three water types is depicted in Table 4.1

Table-4.1: Summarization of Results Comparison of DPSK-DD-Optical OFDM and DPSK-CD-Optical OFDM based on 1×1MIMO and 4×4MIMO systems in three water types.

UOWC systems		**Clear Water**			**Mid Water**			**Turbid Water**		
		Range (m)	BER	P_R (dBm)	Range (m)	BER	P_R (dBm)	Range (m)	BER	P_R (dBm)
DPSK-DD-Optical OFDM	**1×1SISO**	52	3.8×10^{-5}	-11.68	21.3	5.9×10^{-5}	-2	2.4	2.8×10^{-5}	-9.2
	4×4MIMO	131	2.4×10^{-5}	-22	31	3.5×10^{-5}	-8.64	10.5	3.9×10^{-5}	-20.7
DPSK-CD-Optical OFDM	**1×1SISO**	71	2.3×10^{-5}	-28	29.8	4.7×10^{-5}	-21	4.4	1.8×10^{-5}	-29.5
	4×4MIMO	156	3.5×10^{-5}	-42.6	38.5	4.4×10^{-5}	-31.6	12	1.8×10^{-5}	-37.8

The table above clearly shows the performance of the UOWC system with 4×4MIMO is better than the UOWC system with 1×1SISO in the underwater environment in terms of BER and link range, the results showed that spatial diversity manifests its effect as a reduction in fading variance and hence can significantly improve the system performance and increase the viable communication range. And because of increasing the receiver sensitivity to frequency and phase noise, the performance of proposed DPSK-CD-Optical OFDM with 4×4MIMO is better than DPSK-DD-Optical OFDM with 4×4MIMO in the underwater environment in terms of BER and link range.

Finally, a comparison between published works and proposed work is shown in table 4.2.

Table-4.2: A comparison between published works and my work.

Authors	Transmitter type	Light output power (mw)	DSP technique	Data rate	Link range (m)	Water type
[15]	405nm LED	100mw	QAM-DD-OFDM	968 Mbps	2	Turbid
[16]	450nm LD	15 mw	16-QAM-OFDM	4.8Gbps	5.4	Clear
[17]	450nm LED	100mw	64-QAM-DD-OFDM	127.07 Mbps	40	Coastal
[18]	521nm LD	6 mw	256-QAM-DD-OFDM	1.118 Gbps	2	Clear
[19]	450nm LD	30 mw	16-QAM-DD-OFDM	9.6 Gbps	8	Clear
[20]	450nm LD	100mw	16-QAM-CD-OFDM	8.8 Gbps	10	Coastal
[21]	457nm LED	85mw	QAM-DD-OFDM-2×2MIMO	33.6 Mbps	2-5	Turbid
[22]	532nm LD	25-100 mw	OOK-3×1MISO	(0.5-50) Gbps	11-25	Coastal
[23]	450nm LD	100mw	16-QAM-DD-OFDM	(5.2-12.4) Gbps	10.2-1.7	Clear
[25]	521nm LED	85mw	64-QAM-DMT-2×2MIMO	2.175Gbps	1.3	Clear

[27]	532nm LED	80mw	QAM-OFDM-2×2MIMO	7.8Gbps	4	Turbid
[28]	532nm LED	75 mw	QAM-DD-OFDM-2×2MIMO	10 Gbps	2.2	Turbid
Proposed Work	450nm LD	100 mw	DPSK-DD-OFDM-4×4MIMO	10Gbps	131 31 10.5	Clear Mid Turbid
			DPSK-CD-OFDM-4×4 MIMO		156 38.5 12	Clear Mid Turbid

From the above table, we note that it is obvious that there is an improvement in the performance of the UOWC system in terms of increasing link range compared with previous and equivalent studies for the same entries and parameters used in this study

CHAPTER FIVE

CONCLUSIONS and SUGGESTIONS for FUTURE WORKS

5.1 Conclusions

According to the obtained results, the researcher has come up with the following conclusions:

1. From many architectures being proposed in this study for UOWC (such as DPSK-DD-Optical OFDM and DPSK-CD-Optical OFDM), the use of coherent detection Optical OFDM is particularly interesting for enabling the next generation underwater communication systems for its ability to transmit high data rate and overcome underwater impairments (absorption, scattering, and multipath).
2. DPSK-CD-Optical OFDM depicts the best performance of receiver sensitivity compared with DPSK-DD-Optical OFDM. Because of the receiver of DPSK-DD-Optical OFDM is not sensitive to phase, frequency, and polarization like DPSK-CD-Optical OFDM.
3. A SISO system configuration can only send or receive a single signal stream, while a MIMO system can send and receive multiple signals, and can therefore distinguish the signals sent from different transceivers. Since the MIMO system enables more data to be transmitted, issues associated with channel impairments can be solved (such as physical obstructions and turbulence), therefore the occurrence of errors is minimized. From simulation results, the highest allowable range for good links could be enhanced, especially for 4×4MIMO and 1×4SIMO if compared to 1×1SISO, 2×1MISO, 4×1MISO, 1×2SIMO, and 2×2MIMO.

4. The study has led to the proposes and improvement of the UOWC system. Some of the existing issues such as underwater impairments (absorption and scattering) have been identified and suitable solutions have been suggested such as DPSK-CD-Optical OFDM with 4×4MIMO technique.

5. The simulation result of reliable link range at target BER (10^{-5}) for DPSK-DD-Optical OFDM with 4×4MIMO are 10.5m, 31m, and 131m for turbid, mid, and clear water receptively. The simulation result of reliable link range at target BER (10^{-5}) for proposed DPSK-CD-Optical OFDM with 4×4MIMO are 12m, 38.5m, and 156m for turbid, mid, and clear water receptively.
6. Finally, simulation results of UOWC using proposed DPSK-CD-Optical OFDM and MIMO technique led to greater improvement in all UOWC performance especially in terms of data rate and link range.

5.2 Suggestions for Future Works

The following further studies might be suggested:

1. Different modulation, such as Differential Quadrature Phase Shift Keying (DQPSK), can also be considered with UOWC system in future work.
2. To mitigate the PAPR in Optical OFDM systems, PAPR reduction techniques can be exploited for IM/DD and coherent detection system. PAPR mitigation methods such as selective mapping, interleaving, and partial transmit sequence will further enhance the optical OFDM systems performance.
3. Using Dense Wavelength Division Multiplexing (DWDM) technique with optical OFDM in the UOWC system to increase the system capacity.
4. Using Dual Polarization Multiplexing (DPM) technique with optical OFDM-MIMO in the UOWC system to increase the data rate.

REFERENCES

[1] X. Zhang, J. H. Cui, S. Das, M. Gerla, and M. Chitre, "Underwater Wireless Communications and Networks: Theory and Application: Part 2 [Guest Editorial]," IEEE Commun. Mag., vol. 54, no. 2, pp. 30–31, 2016.

[2] M. Al-rubaiai, "DESIGN AND DEVELOPMENT OF AN LED-BASED OPTICAL COMMUNICATION SYSTEM," Michigan State University, 2015.

[3] Rabee M. Hagem, "Real Time Evaluation of Swimmers Performance Based on an Optical Wireless Communication System," Griffith University, 2013.

[4] H. Kaushal and G. Kaddoum, "Underwater Optical Wireless Communication," IEEE Access, vol. 4, pp. 1518–1547, 2016.

[5] W. Dargie and C. Poellabauer, "'Fundamentals of Wireless Sensor Networks,'" First edit. A John Wiley and Sons, Ltd., Publication, 2010.

[6] M. Massot-Campos and G. Oliver-Codina, "Optical sensors and methods for underwater 3D reconstruction," Sensors (Switzerland), vol. 15, no. 12, pp. 31525–31557, 2015.

[7] J. Bayarri, "Contribution to Research on Underwater Sensor Networks Architectures by Means of Simulation," politecnica university, 2013.

[8] N. Klausner, "Underwater Target Detection Using Multiple Disparate Sonar Platforms," Colorado State University, 2010.

[9] H. D. Trung and N. Van Duc, "An analysis of MIMO-OFDM for underwater communications," Int. Congr. Ultra Mod. Telecommun. Control Syst. Work., 2011.

[10] B. Tian, F. Zhang, and X. Tan, "Design and development of an LED-based optical communication system for autonomous underwater robots," 2013 IEEE/ASME Int. Conf. Adv. Intell. Mechatronics Mechatronics Hum. Wellbeing, AIM 2013, pp. 1558–1563, 2013.

[11] P. A. McGillivary, V. Chirayath, and J. Baghdady, "Use of multi-spectral high repetition rate LED systems for high bandwidth underwater optical

communications, and communications to surface and aerial systems," 2018 4th Underw. Commun. Netw. Conf. UComms 2018, pp. 1–5, 2018.

[12] J. Wang, C. Lu, S. Li, and Z. Xu, "100 m/500 Mbps underwater optical wireless communication using an NRZ-OOK modulated 520 nm laser diode," Opt. Express, vol. 27, no. 9, p. 12171, 2019.

[13] X. S. Oubei, H. M., "Scintillations of RGB laser beams in weak temperature and salinity-induced oceanic turbulence," 2018 Fourth Underw. Commun. Netw. Conf. (UComms), Underw. Commun. Netw. Conf. (UComms), 2018 Fourth, p. 1, 2018.

[14] B. Majlesein, A. Gholami, and Z. Ghassemlooy, "A Complete Model for Underwater Optical Wireless Communications System," 2018 11th Int. Symp. Commun. Syst. Networks Digit. Signal Process. CSNDSP 2018, no. July, 2018.

[15] I. Mizukoshi, N. Kazuhiko, and M. Hanawa, "Underwater optical wireless transmission of 405nm, 968Mbit/s optical IM/DD-OFDM signals," in 2014 OptoElectronics and Communication Conference and Australian Conference on Optical Fibre Technology, 2014, pp. 216–217.

[16] H. M. Oubei et al., "4.8 Gbit/s 16-QAM-OFDM transmission based on compact 450-nm laser for underwater wireless optical communication," Opt. Express, vol. 23, no. 18, p. 23302, 2015.

[17] J. Xu et al., "OFDM-based broadband underwater wireless optical communication system using a compact blue LED," Opt. Commun., vol. 369, pp. 100–105, 2016.

[18] J. Xu et al., "Underwater Laser Communication Using an OFDM-Modulated 520-nm Laser Diode," IEEE Photonics Technol. Lett., vol. 28, no. 20, pp. 2133–2136, 2016.

[19] H. Lu et al., "An 8 m/9.6 Gbps underwater wireless optical communication system," IEEE Photonics J., vol. 8, no. 5, pp. 1–7, 2016.

[20] C.-M. Ho et al., "A 10m/10Gbps underwater wireless laser transmission system," in Optical Fiber Communication Conference, 2017, pp. Th3C-3.

[21] Y. Song et al., “Experimental demonstration of MIMO-OFDM underwater wireless optical communication,” Opt. Commun., vol. 403, no. April, pp. 205–210, 2017.

[22] M. V. Jamali, J. A. Salehi, and F. Akhoundi, “Performance studies of underwater wireless optical communication systems with spatial diversity: MIMO Scheme,” IEEE Trans. Commun., vol. 65, no. 3, pp. 1176–1192, 2017.

[23] T. C. Wu and Y. C. Chi, “Blue laser diode enables underwater communication at 12.4 gbps,” Sci. Rep., vol. 7, no. August 2016, pp. 1–10, 2017.

[24] I. C. Lu and Y. L. Liu, “205 Mb/s LED-based underwater optical communication employing OFDM modulation,” 2018 Ocean. - MTS/IEEE Kobe Techno-Oceans, Ocean. - Kobe 2018, vol. 1, pp. 1–4, 2018.

[25] F. Wang, Y. Liu, F. Jiang, and Nan Chi, “High speed underwater visible light communication system based on LED employing maximum ratio combination with multi-PIN reception,” Opt. Commun., vol. 425, no. December 2017, pp. 106–112, 2018.

[26] A. Huang, L. Tao, and Q. Jiang, “Ber performance of underwater optical wireless MIMO communications with spatial modulation under weak turbulence,” in 2018 OCEANS-MTS/IEEE Kobe Techno-Oceans (OTO), 2018, pp. 1–5.

[27] A. Amantayeva, M. Yerzhanova, and R. C. Kizilirmak, “Multiuser MIMO for Underwater Visible Light Communication,” Proc. 2nd Int. Conf. Comput. Netw. Commun. CoCoNet 2018, pp. 164–168, 2018.

[28] Y. Li, H. Qiu, X. Chen, J. Fu, J. Wang, and Y. Zhang, Optimization of Optical Imaging MIMO-OFDM Precoding Matrix for Underwater VLC, vol. 11637 LNCS. Springer International Publishing, 2019.

[29] H. M. Oubei, “Underwater Wireless Optical Communications Systems : from System- Level Demonstrations to Channel Modeling,” King Abdullah University of Science and Technology, 2018.

[30] H. Brundage, “Designing a Wireless Underwater Optical Communication System,” Massachusetts Institute of Technology February, 2010.

[31] S. HRANILOVIC, Wireless Optical Communication Systems. Springer, 2004.

[32] H. M. Oubei, C. Li, K.-H. Park, T. K. Ng, M.-S. Alouini, and B. S. Ooi, “2.3 Gbit/s underwater wireless optical communications using directly modulated 520 nm laser diode,” Opt. Express, vol. 23, no. 16, p. 20743, 2015.

[33] A. HRAGHI, “Application of Mach-Zehnder Modulator for High Speed Optical Communication Network,” Telecom ParisTech, 2016.

[34] T. Rahman, “Flexible and high data-rate coherent optical transceivers,” Eindhoven university of technology, 2017.

[35] Xiaoyong Chen, “Design and Otimization of Optical Fiber Based PSK Demodulation for High bit rate optical networks,” 2015.

[36] F. Xiong, “‘Digital Modulation Techniques,’” vol. 53, no. 9. 685 Canton Street,Norwood,MA 02062: ARTECH HOUSE, INC., 2000.

[37] F. Jacobsson, “DPSK modulation format for optical communication using FBG demodulator DPSK modulation format for optical communication using FBG demodulator,” 2004.

[38] Z. Zeng, S. Fu, H. Zhang, Y. Dong, and J. Cheng, “A Survey of Underwater Optical Wireless Communications,” IEEE Commun. Surv. Tutorials, vol. 19, no. 1, pp. 204–238, 2017.

[39] L. K. Gkoura et al., “Underwater optical wireless communication systems: A concise review,” in Turbulence Modelling Approaches - Current State, Development Prospects, Applications, InTech, 2017.

[40] I. E. Karametou, “Theoretical study and simulation of Underwater Wireless Optical Communications channels with diffused light transmissions in the visible spectrum,” 2017.

[41] C. Gussen and P. Diniz, “A Survey of Underwater Wireless Communication Technologies,” J. Commun. Inf. Syst., vol. 31, no. 1, pp. 242–255, 2016.

[42] G. Baiden, Y. Bissiri, and A. Masoti, “Paving the way for a future underwater omni-directional wireless optical communication systems,” Ocean Eng., vol. 36, no. 9–10, pp. 633–640, 2009.

[43] S. Jaruwatanadilok, “Underwater wireless optical communication channel modeling and performance evaluation using vector radiative transfer theory,” IEEE J. Sel. Areas Commun., vol. 26, no. 9, pp. 1620–1627, 2008.

[44] L. J. Johnson, F. Jasman, R. J. Green, and M. S. Leeson, “Recent advances in underwater optical wireless communications,” Underw. Technol., vol. 32, no. 3, pp. 167–175, 2014.

[45] S. Arnon and D. Kedar, “Non-line-of-sight underwater optical wireless communication network,” J. Opt. Soc. Am. A, vol. 26, no. 3, p. 530, 2009.

[46] E. Zedini, H. M. Oubei, A. Kammoun, M. Hamdi, B. S. Ooi, and M. S. Alouini, “Unified Statistical Channel Model for Turbulence-Induced Fading in Underwater Wireless Optical Communication Systems,” IEEE Trans. Commun., vol. 67, no. 4, pp. 2893–2907, 2019.

[47] K. Kaur, R. Miglani, and J. S. Malhotra, “The Gamma-Gamma Channel Model - A Survey,” Indian J. Sci. Technol., vol. 9, no. 47, pp. 10–13, 2016.

[48] W. S. and I. Djordjevic, OFDM for Optical Communications, vol. book. Elsevier, 2013.

[49] H. Trung and N. Van Duc, “An analysis of MIMO-OFDM for underwater communications,” Int. Congr. Ultra Mod. Telecommun. Control Syst. Work., vol. 1234, no. 89, p. 5, 2011.

[50] A. Khaled, “High Data Rate Coherent Optical Ofdm System for Long Haul Transmission,” University of Denver, 2013.

[51] S. Hamid, “Performance Evaluation of Optically Preamplified M-ary PPM Systems for Free-Space Optical Communications,” J. Chem. Inf. Model., vol. 53, no. 9, pp. 1689–1699, 2019.

[52] A. S. AL SHANTTi, “Optical Orthogonal Frequency Division Multiplexing Direct Detection for Improving Capacity of Radio over Fiber Transmission System,” The Islamic University of Gaza, 2012.

[53] H. Ali, “Modeling and Simulation of High Speed Optical Fiber Communication System with OFDM,” College of Physical Science & Technology Central China Normal University, 2015.

[54] W. Shieh, H. Bao, and Y. Tang, “Coherent optical OFDM: theory and design,” Opt. Express, vol. 16, no. 2, p. 841, 2008.

[55] N. Mansor and A. Aloff, “Coherent OFDM for Optical Communication systems Submitted,” The Islamic University - Gaza, 2014.

[56] A. Y. Fattah and F. H. Abdul-baqi, “Polarization Division Multiplexing Coherent Optical OF DM Transmission Systems,” IJCCCE, vol. 15, no. 3, pp. 64–76, 2015.

[57] N. Und, “Investigation of Receiver Concepts for Coherent Optical Orthogonal Frequency Division Multiplexing Communication Systems,” 2014.

[58] B. Zid and R. Kosai, “Multi User MIMO Communication: Basic Aspects, Benefits and Challenges,” Recent Trends Multi-user MIMO Commun., pp. 3–24, 2013.

[59] S. Yadav and V. Kumar, “Optimal Clustering in Underwater Wireless Sensor Networks: Acoustic, em and FSO Communication Compliant Technique,” IEEE Access, vol. 5, no. c, pp. 12761–12776, 2017.

[60] W. Liu, “The End-to-End BER Analysis of Two Simulated OFDM-RoF Systems,” University of Waterloo, 2015.

[61] M. Abraham, “Analysis of Underwater Environment and Establishment of Underwater Wireless Optical Communication link,” EuroJournals Publ., vol. 87, no. April 2017, pp. 349–358, 2012.

الملخص

يمكن الاستفادة بشكل كبير من الاتصالات اللاسلكية البصرية تحت الماء أنظمة (UOWC) في ضوء المتطلبات المتزايدة لنقل البيانات بسرعة عالية كتلك المستخدمة في العديد من التطبيقات. لهذا السبب ،كان تطوير انظمة (UOWC) جديدة وتحسين الانظمة الحالية مجالا بحثيا شائعا للغاية في العقود الماضية . وفي هذا السياق الهدف من هذه الرسالة هو دراسة تصميم وتحليل اداء لنظام للجوانب الفيزيائية لـ (UOWC) باستخدام طرق تضمين مختلفة وتحت قنوات مائية مختلفة.

بحثت الدراسة في انظمة اتصالات بصرية لاسلكية مختلفة تحت الماء والتي تستخدم تضمين DPSK مع تقنيات الكشف المباشر (DD) مع تكنولوجيا مضاعفة التقسيم الترددي المتعامد البصري (Optical-OFDM), تضمين DPSK مع الكشف المتماسك (CD) مع تكنولوجيا مضاعفة التقسيم الترددي المتعامد البصري (Optical-OFDM), والتقنيتين السابقتين مستندة الى تقنية الادخال المتعدد والاخراج المتعدد (MIMO) (1×1SISO,1×4 SIMO,1×2 SIMO,2×1 MISO,4×1 MISO, 2×2 MIMO and 4×4 MIMOعلى التوالي) لتحسين حساسية المستلمة وزيادة مدى الارسال.

تم استخدام الحقيبة البرمجية optisystem™ (Ver. 16.0.0) في عملية محاكاة ل (DPSK-DD-Optical OFDM) و(DPSK -CD-Optical OFDM) مع استخدام تقنية متعدد المدخلات متعدد المخرجات (MIMO) المقترحة.

نتائج المحاكاة التي تم الحصول عليها اظهرت ان استخدام (DPSK-CD-Optical OFDM) افضل من (DPSK-DD-Optical OFDM) باستخدام 4×4MIMO لمدى الاتصال الموثوق عند معدل خطأ البيانات المستهدف (10^{-5}) والذي يعتبر اقل من عتبة عملية تصحيح الاخطاء(FEC 10^{-3}) .

على سبيل المثال مع استخدام (DPSK-DD-Optical OFDM)مع 4×4MIMO هي 10.5 مترا و 31 مترا و131 مترا للمياة العكرة ومتوسطة العكورة والنقية على التوالي. ونتائج المحاكاة باستخدام (DPSK-CD-Optical OFDM) مع 4×4MIMO هي هي 12 مترا و 38.5 مترا و156 مترا للمياة العكرة ومتوسطة العكورة والنقية على التوالي.

علاوة على ذلك، خلصت الرسالة بنتائج المحاكاة لنظام UOWC باستخدام التقنية المقترحة اظهرت تحسن افضل مقارنة بالبحوث السابقة عند نفس معاملات الادخال.

جمهورية العراق

وزارة التعليم العالي والبحث العلمي

جامعة الفرات الاوسط التقنية

الكلية التقنية الهندسية– نجف

بحث في أداء الاتصالات الضوئية اللاسلكية تحت الماء تحت تأثيرات تقنيات تضمين مختلفة وتكوين متعدد الادخال متعدد الاخراج

رسالة مقدمة الى
قسم هندسة تقنيات الاتصالات
كجزء من متطلبات نيل درجة ماجستير تقني في هندسة الاتصالات

تقدم بها

منذر نعمان حسن

بكالوريوس في هندسة تقنيات الاتصالات

إشراف

الاستاذ المساعد الدكتور

احمد غانم وداي

ايلول/ 2020